x

The expression and purification of zinc metalloprotease STE24 (ZMPSTE24) and study of the interactions between the protein-inhibitor binding

By

Mengjin Gao

A thesis submitted to McGill Univeristy in partial fulfilment of the requirement of the requirements of the degree of Master of Science

Table of Content

Abstract

The proteins which contain C-terminal “CaaX” motifs are often post-translationally modified by prenylation, examples include the zinc metalloproteases yeast Ste24p and the human ZMPSTE24. Prelamin A is the precursor of the filament protein lamin A, which is the only substrate of ZMPSTE24. ZMPSTE24 cleaves prelamin A twice during the process of lamin A maturation. Mutations in the ZMPSTE24 cleavage site of prelamin A causes the progeria syndrome. However temporary inhibition of ZMPSTE24 has been shown to block cell mitosis and proliferation, and proposed as a novel mechanism for cancer chemotherapy. The ZMPSTE24 is known to be inhibited by the off-target effect of some HIV protease inhibitors such as Lopinavir. In order to develop new more potent and selective ZMPSTE24 inhibitors, we cultivated yeast cells to express the transmembrane protein of human recombinant ZMPSTE24, purify the protein ZMPSTE24, and analyzed the purity of the enzyme by mass spectrometry.

Résumé

Les protéines qui contenaient des motifs «CaaX» C-terminaux sont catalysées et modifiées post-traductionnellement par des métalloprotéases de zinc telles que Ste24p ou ZMPSTE24. La prélamine A est le précurseur de la protéine de filament lamin A qui est le seul substrat de ZMPSTE24. ZMPSTE24 clive ses substrats deux fois au cours du processus de maturation de la lamine A. Des mutations dans le gène ZMPSTE24 ou bloquant l'activité de ZMPSTE24 provoqueraient le syndrome de la progeria et inhiberaient la mitose et la prolifération des cellules. Le ZMPSTE24 est connu pour être inhibé par l'effet hors cible des inhibiteurs de protéase du VIH. Certains inhibiteurs de la protéase du VIH tels que le lopinavir peuvent faiblement bloquer l'activité de ZMPSTE24. Les nouveaux inhibiteurs spécifiques de ZMPSTE24 ont été synthétisés et analysés l'affinité entre les interactions protéine-médicament. Ici, nous avons cultivé des cellules de levure pour exprimer la protéine transmembranaire ZMPSTE24, purifier la protéine ZMPSTE24 et analyser l'enzyme de pureté existante par analyse par spectrométrie de masse. En tant que protéine transmembranaire, la ZMPSTE24 humaine n'est pas stable après les étapes de purification.

Acnowledgement

I would like to thank Dr. Youla S. Tsantrizos for offering me a position in her lab and for giving me an interesting project that lined up my interest in structural biology and drug discovery research. Thank you for providing me invaluable insight and advice throughout past year I spent here. Additionally, I would like to thank my Research Advisory Committee and collaborators, Dr. Jean-François Trempe and Dr. Albert M. Berghuis for their strongly support and direction during my graduate studies. I would also like to thank Dr. Christopher Thibodeaux to help and teach me the process of protein purification. At the same time, I want to thank them for allowing me to use their laboratory to improve my subject.

Thank you for my friends, Andrew Bayne and Christina Gagnon, for always supporting my decisions and guidance me during the process of project research. Thank you for teaching and helping me even when I was not, especially when my life and lab experiments all got to be a little too much for me to handle. Thank you for always encouraging me and believing I could do whatever I put my mind to, even when I did not believe in myself.

Thank you to my family members for encouraging me throughout my education and for continuing to support me for my future life and decisions.

I would like to thank my undergraduate biochemistry teacher, Dr. Mingjun Zhang, for igniting my passion for science and biochemistry.

I would also like to acknowledgement the first mentor I ever had, Dr. Hongsheng Ouyang. You taught me how to think like a scientist and how to ask the right questions. You also encouraged me, had tremendous faith in me, and made me feel like I was cut out for the lab and for graduate school, and for that, I think I will be forever grateful. You are a wonderful mentor and anyone that has the privilege to work closely with you is very lucky.

I would also like to acknowledge the members of the Tsantrizos, Trempe, and Berghuis lab for making the last year easier than they would have been otherwise especially during the experiences of Covid-19. Thank you for the advice when I didn’t know what to do next, for the technical help, and emotional support. I would like to thank Christina for all her help, guidance

and time she took to teach me culture cells and do Western Blotting analysis, and for teaching me how to do most of the techniques included in protein expression and purification steps. I would like to thank Michal Zielinski to teach us how to use fermenter to do protein expression experiments, and I am thankful for Tolou to teach us how to do techniques included in cell lysis steps. I would like to strongly thank to Andrew to teach me how to use the techniques included in protein purification and analysis steps, and he also taught me how to design experiments and how to analyze research results. Thank you to Rebecca for helping me to fix my problems in experiments and gave me suggestions. And last, but definitely not least, thank you to everyone for being so open and willing to welcome me into the lab and your life, for your friendship, your support, and for making me laugh daily. Thank you for always listening and being someone, I could lean on for past graduate studies. Grad school would not have been nearly the same without you.

Preface and contribution of others

I hereby state that I carried out the work presented in this thesis unless state otherwise, analyzed the data, and wrote this thesis. I produced the figures presented. Prof. M. Dumont's group constructed the plasmid which contained the human ZMPSTE24 gene and transferred it into yeast cells. Christina Gagnon and Michal Zielinski expressed the protein and Christina Gagnon did the cell lysis experiments in Prof. A. Berghuis' lab. Andrew Bayne helped in guiding me to do the protein purification experiments and helped me analyze the human ZMPSTE24 by MALDI analysis and in-gel digestion experiments in Prof. J.-F. Trempe's lab. Prof. Y. S. Tsantrizos conceived this project, supervised my work and provided feedback on this thesis.

I feel as though it is necessary for me to state here that my research was heavily disrupted by COVID-19. There are instances when there were gaps in my experiments and times when I was prohibited from working in the lab, due to COVID-19 health safety regulations.

List of figures

List of Abbreviations

AIDS	acquired immunodeficiency syndrome
CTD	C-terminal domain
ddH_2O	deionized distilled water
DDR	DNA damage response
ECM	extracellular matrix
EtOH	ethanol
FTI	farnesyl transferase inhibitor
GGTI	inhibitors of geranylgeranyltransferase
HAART	highly active antiretroviral therapy
hFPPS	farnesyl pyrophosphate synthase
hGGPPS	geranylgeranyl pyrophosphate synthase
HGPS	Hutchinson-Gilford progeria syndrome
HIV	human immunodeficiency virus
HMG-CoA	hydroxymethylglutaryl coenzyme A
ICMT	isoprenylcysteine carboxylmethyltransferase
L5D	Loop 5 domain
M4	thermolysin family of enzymes
PIs	protease inhibitors
PTM	post-translational modification
ZMPSTE24	zinc metalloprotease STE24

1. Literature Review

1.1. Overview

In yeast and other eukaryotic cells, some proteins undergo post-translational modifications (PTMs) in order to complete the process of maturation and become biologically relevant. Isoprenylation is a PTM which is important for the modification of CAAX motif (C=cysteine, A=aliphatic amino acid, X=any amino acid). [1] Many proteins contain the CAAX motif at their C-terminus and perform various cellular functions throughout the body. [2] The prenyl transferase enzymes catalyze the isoprenylation step and the modified target protein can also undergo several other processing steps after the isoprenylation step. [1] The isoprenylation of the CAAX is modified by either the farnesyl group (C15) or the geranylgeranyl group (C20) on the cysteine residue. [3]

The M48 family of proteins (which contain an CAAX motif) are known to participate in some signalling pathways (such as the p53 signalling pathway), cell proliferation, and the step of mitosis during cell division. [4] These proteins are also considered to be associated with some diseases, such as progeria, cancer and mandibular dysplasia. The human zinc metalloprotease STE24 (ZMPSTE24) is the enzyme responsible for cleaving the prenylated precursor of lamin A. [5] My project is focused on the expression and purification of ZMPSTE24 from yeast.

1.2. M48 family protease

Proteases, also known as proteinases or proteolytic enzymes, are a class of enzymes that catalyze the cleaving of proteins via the hydrolysis of an amide bond. Proteases can be classified in two general types, exopeptidases and endopeptidases. The exopeptidases can cleave N- or C-terminal peptide bonds, whereas the endopeptidases break internal bonds. [6] According to proteolytic mechanism, proteases are divided into six broad groups, and metalloproteases are one of these six classes. The catalyst mechanism of metalloproteases involves a metal ion that coordinates the substrate in the active site and may help to activate a water molecule, which can then act as a nucleophile and attack the carbonyl carbon of a peptide bond. [7] Zinc ion is found in the active sites of many metalloenzymes. In the activation mechanism of these metalloproteases,

the zinc ion is coordinated by three residues and it activates the water molecule. Zinc ions can act as Lewis acids to participate in the catalytic reaction. A unique signature of zinc metalloproteases family is the HEXXH (His-Glu-any-any-His) motif, which has been found and identified in the catalytic site of this type of metalloproteases (zinc metalloprotease), such as thermolysin, surface protease, aminopeptidase N, peptidase N, neutral protease, stromlysin and gelatinase, etc. [8]

M48 family proteases are metalloproteases with HEXXH motif (having the two histidine-zinc-ligands coordination's) and an adjacent glutamate on the next helix being the third ligand to coordinate the zinc ion. Until 2007, over 200 protein sequences had been determined to belong to this family. [9] These proteins typically folds to form a deep groove/cleft into which the substrate peptide can bind. [10] There are three subgroups in M48 family of proteins, M48 A, M48 B and M48 C. The yeast enzyme Ste24p belong to M48 A subgroup and is produced by *Saccharomyces cerevisiae*; ZMPSTE24 is its mammalian ortholog and plays a very important role in the maturation of the nuclear structural protein lamin A.

1.3. Thermolysin

1.3.1. Overview of Thermolysin

Thermolysin is a type of thermostable neutral metalloprotease. The thermolysin family enzymes are also called as M4 family metalloproteases, and thermolysin from *Bacillus thermoproteolyticus* is one of the classic M4 family metalloproteases. The M4 family has over 200 types of protein sequences, which are all found in bacteria. [9] M4 family enzymes are all zinc metalloproteases that bind a single catalytic zinc ion on their active site. Members in M4 family of enzymes participated in the degradation of extracellular proteins.

Thermolysin from *Bacillus thermoproteolyticus* is a 34.6 kDa protein and was the first metalloprotease to be crystalized and structurally characterized. [11] The optimal pH for catalytic activity of this enzyme is around pH7.0. [12] In structural research and medicinal chemistry, thermolysin has been used as a prototypical model for the design of inhibitors that target mammalian zinc metalloproteases.

1.3.2. The basic structure of thermolysin

In 1972, the first crystal structure of thermolysin was reported, in high resolution (2.3 Å), [13] and subsequently, several co-crystal structures of thermolysin were reported with inhibitors bound to its active site (Figure. 1A). [11, 14] For example, Hausrath and Matthews reported a co-crystal structure with a dipeptide bound in the active site. [15] The substrate and inhibitor specificity of thermolysin was also investigated by selecting different types of peptide substrates and peptidomimetic inhibitors. [16] For example, the interaction of these ligands with the S1' pocket of the enzyme were shown to be the major specificity site for binding of large hydrophobic residues. [17] Thermolysin can cleave peptides and proteins at N-terminal side of residues, such as Leu, Phe, Ile, and Val. [18] Although the natural substrates of thermolysin can also interact with residues in the S1 and S2 subpockets of the active site, these interactions are less important that the S1' binding sub-pocket.

The protein of thermolysin has a length of 316 amino acid residues (34.6 kDa). As expected, the Zn^{2+} ion is bound within two histidine side chains of the His-Glu-Leu-Thr-His (HELTH) motif (residues 142-146). [16] Additionally, the Zn^{2+} ion also interacts with the Glu166 residue which is located at C-terminal side to the motif and a water molecule, to form a tetrahedral structure within the activate the active site of enzyme (Fig. 1C).The catalytic activity of thermolysis is completely lost in the absence of the Zn^{2+} ion, however, the enzyme can maintain activity if the Zn^{2+} ion is replaced with stoichiometric amounts of Co^{2+}, Mn^{2+} , or a high molar excess of Fe^{2+} ions. [19] The structural changes of zinc replacement in the active site of enzyme thermolysin have been confirmed by X-ray crystallography. [20] There are also four calcium atoms that can bind to thermolysin. [21] Two calcium atoms are located at a double binding site around the active site cleft. The rest of the two calcium atoms are located at an exposed loops in the N and C-terminal domains respectively. [22] There is no known catalytic role for the four calcium atoms, but they are related to the stability of enzyme to likely protect it from autolysis. [20] These calcium ions can be replaced by other metal ions such as lanthanide ions. [23] It is noteworthy that more recently, the X-ray structures of the yeast Ste24p and the human ZMPSTE24 were shown to be very similar to that of thermolysis in the active sites region. [10, 24, 25]

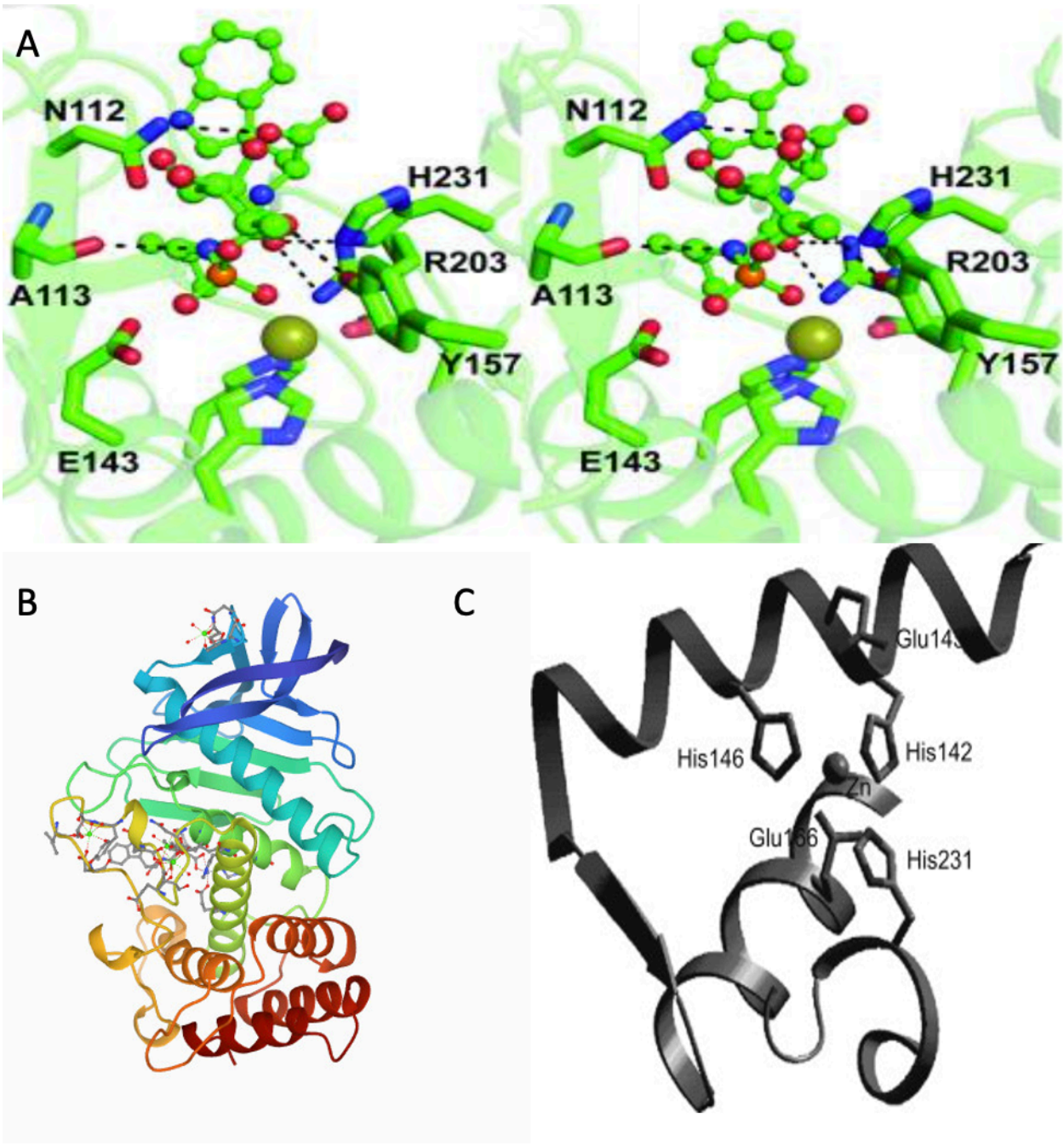

Figure 1. Crystal structure and the active site of thermolysin. (**A**) The phosphoramidon-binding specificity pocket of thermolysin. [26] [PDB ID 1TLP]. (**B**) Crystal structure of thermolysin determined by x-ray crystallography. [PDB ID 1TMN]. (**C**) The active site of thermolysin. [16] The zinc ion is coordinated with two histidines in His- Glu- Leu- Thr- His (HELTH) zinc binding motif (residues 142-146) as zinc ligands. Another glutamine (Glu166) and a water molecule provide other zinc ligands. The zinc ion in the active site is coordinated with 4 ligands to form the tetrahedral geometry structure to catalyze substrates.

1.3.3. Catalytic mechanism of thermolysin

The general catalytic mechanism was first proposed for the zinc peptidase family, based on the glutamate of the HELTH sequence, which polarizes a water molecule that is coordinated to Zn^{2+} ion. The activated water molecule then attacks the scissile amide bond of the peptidic substrate. A histidine residue (His231) contributes to the stability of transition state in the active site of thermolysin. [11, 27] In 1995, Beaumont's group investigated the roles of residues within the active site by mutating each residues in thermolysin. [28] The drastic decrease in the activity of the enzyme were observed after mutation of His231 in thermolysin. Kubo and Toma group also reported the importance of Glu143 and His231 by mutating the residues resulted in decrease in the stability and activity of enzyme thermolysin. [29, 30] Matthews and co-workers later proposed a hydrolysis mechanism for thermolysin. [20]The currently preferred catalytic mechanism of thermolysin is supported by crystallographic and biological studies. The zinc ion in the active site of thermolysin has two roles: (a) it polarizes the carbonyl group of the substrate and (b) facilitates deprotonation of the water nucleophile. The enzyme catalyzes cleavage of substrate bonds through the general-base type mechanism with attack of a water molecule or hydroxide ion on the carbonyl carbon of the scissile peptide bound. The nucleophilicity of the water molecule is increased by having two hydrogen-bonds with Glu143, and its oxygen coordinated with the zinc ion. The nucleophilic attack is aligned by the tripartite interactions, which would leave the remaining lone pair directed toward the carbonyl carbon of the substrate. By the effects of zinc ion and glutamate residue, the water molecule then attacks the carbonyl carbon to form a pentacoordinate intermediate. The proton can be accepted by Glu143, transferring the proton to the leaving nitrogen (Fig. 2). The side chain oxygen of Asn112 and the carbonyl of Ala113 form hydrogen bonds from the protonated nitrogen of the scissile bond. The interactions are showed carbobenzoxy-Phe (P)-Leu-Ala (ZF(P)LA) as the scissile scaffold of a thermolysis inhibitor (Fig. 2). Other tight-binding inhibitors of thermolysin can mimic the structure of tetrahedral intermediate to block the activity of the enzyme for therapeutic or research applications. The second proton is transferred through Glu143 to participate in the collapse of the intermediate. During the process, the proton is accepted from the hydrated peptide and shuttled to the leaving nitrogen. The residue His231 helps stabilize the transition state by donating a hydrogen bond to the hydrated peptide.The catalytic mechanism

of thermolysin is similar to that of the zinc metalloprotease STE24 (ZMPSTE24), and will be described in the later part of thesis.

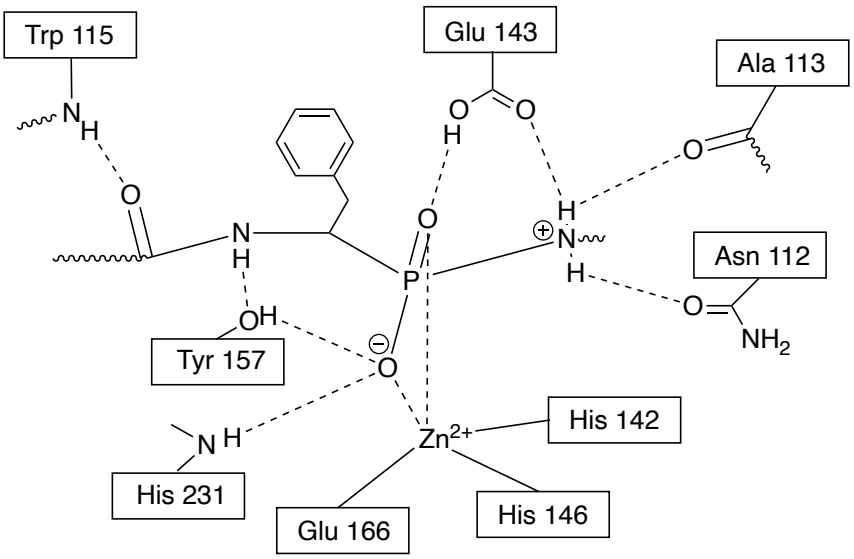

Figure 2. The proposed catalytic mechanism of thermolysin. The interaction of ZF(P)LA with thermolysin. The ZF(P)LA sequence is a scissile inhibitor as an example for the tight -binding inhibitor design.

1.3.4. Inhibitors of thermolysin

Thermolysin is often used in drug discovery as a model zinc metalloprotease to design inhibitors for such enzymes. [10, 31] Thermolysin is strongly blocked by zinc-chelating agents such as 1,10-phenanthroline and EDTA (Fig. 3A). [19] Also, thermolysin is blocked by phosphoramidon which binds specificaly to the S1′ and S2′ sub-pockets of the active site (Fig. 3B). [26] Phosphoramidon is membrane metallo-endopeptidase inhibitor that inhibits the activity of enzyme thermolysin. The specific thermolysin inhibitors are mostly peptide substrate homologs, which allowed hydrophobic residue to fit in the different subsites of thermolysin and strongly bind to the Zn^{2+} ion. Modeling of the sequence similarity between thermolysin and new zinc metalloprotease enzymes can be used to determine the structure of the new enzymes. The members of M48 family proteases are expected to have highly similar three-dimensional structures. [32]

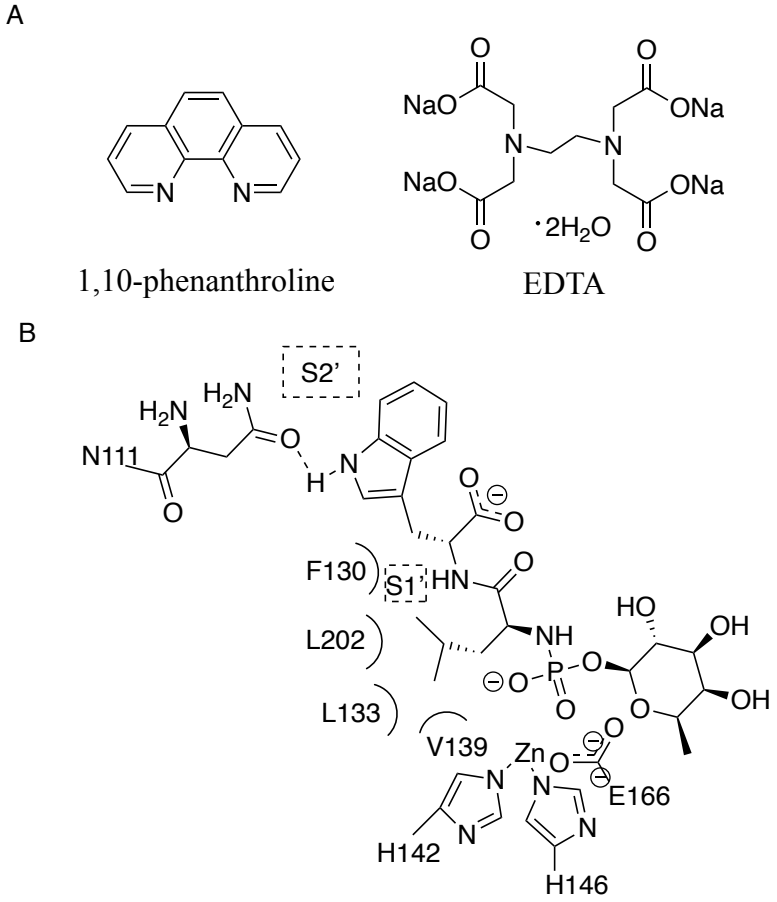

Figure 3. Inhibitors of thermolysin. (**A**) Chemical compounds, 1,10-phenanthroline and EDTA can block the activity of thermolysin. (**B**) The mechanism of thermolysin inhibitor phosphoramidon. The residues responsible for forming the specificity pockets for residues immediately C-terminal to the scissile bond (S1′) and C-terminally distal to the scissile bond (S2′) as present. [26]

1.4. Ste24p

The yeast protein Ste24p is an integral membrane protein which is involved in the proteolytic maturation of the isoprenylated precursor of **a**-factor protein in *Saccharomyces cerevisiae.* [33] The precursor of a-factor is a 36-residue peptide, and the length of this peptide affects the cleavage efficiency of the enzyme (Figure 5). Dumont's group found that the zinc ion is essential for the

catalytic activity of Ste24p, and that this enzyme is anchored in the ER membranes of yeast cells. In 2013, Dumont's group also reported the first X-ray crystal structure of Ste24p, which was isolated from *Saccharomyces mikate* (Smste24p) (Figure 4). The overall structure of Ste24p is composed of seven transmembrane helices that constructed a big inner cavity, which contains the active site.

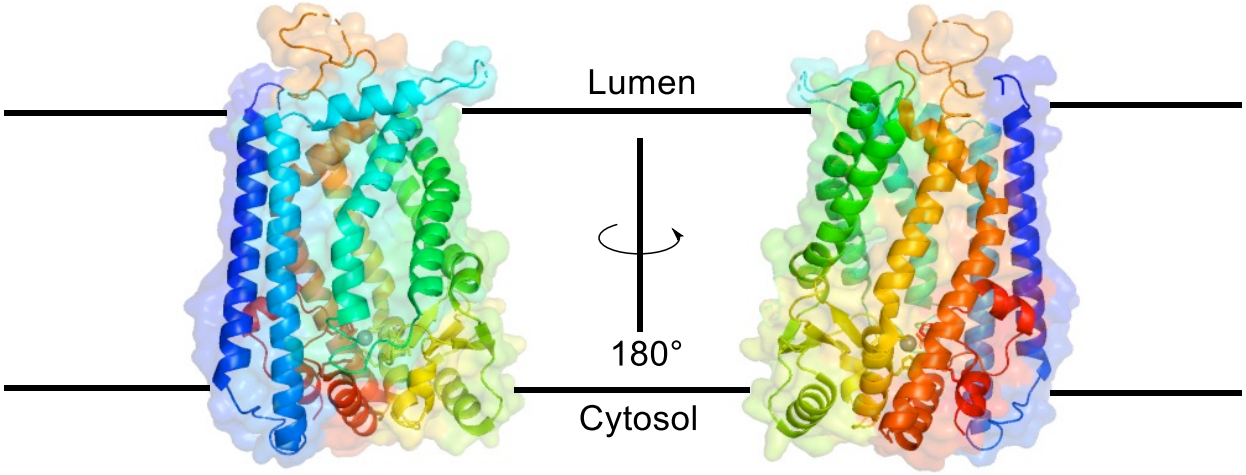

Figure 4. Crystal structure of SmSte24p. [PDB ID 4IL3]. Pronounced kinks in helices III (cyan) and VII (red) are visible. The structure is colored from blue to red from N- to C-terminus. The Zn^{2+} is represented as a grey sphere.

Ste24p was thought to be the only enzyme that could catalyze cleavage of the isoprenyl substrate of this enzyme, [33] however, new evidences revealed that the isoprenyl moiety is not absolutely required for substrate recognition and that the enzyme can cleave both the prenylated and the non-prenylated substrate, the precursor of a-factor. [34] Interestingly, before the X-ray structures of both the yeast enzyme Ste24p and human enzyme ZMPSTE24 were reported, it was already shown that Ste24p can cleave both the **a**-factor peptide the human prelamin A protein, suggesting a high similarity between structures of the two enzymes (i.e., Ste24p and ZMPSTE24). [35]

1.5. ZMPSTE24

The human zinc metalloprotease STE24 (ZMPSTE24) is a homolog of Ste24p, and critically important for the proteolytic maturation of lamin A from its precursor protein, the farnesylated prelamin A. [36] The prenyl group of prelamin A is attached to cysteine residue of the C-terminal CAAX motif by farnesyl transferase. Prelamin A is the only substrate of ZMPSTE24, and ZMPSTE24 plays an important role in the maturation of lamin A. [37] The farnesylation of prelamin A is thought to be the target to help ZMPSTE24 to bind its substrate prelamin A. [38] Prelamin A undergoes four catalytic post-translational modifications before mature lamin A is formed. The first step is the prenylation/farnesylation step. In the second step, involves cleaving of the last three amino acid residues (AAX) from the C-terminus of prelamin A, a process catalyzed by either ZMPSTE24 or the Ras converting enzyme (Rce1, which is responsible for the processing of Ras and the G-alpha subunit of heterotrimeric G proteins). [39] Then, the enzyme isoprenylcysteine carboxylmethyltransferase (ICMT) catalyzes the carboxymethylation of the free C-terminus in the substrate. [40] In the final modification step involves cleaving of the C-terminal 15 amino acids of prelamin A (including the prenylated cysteine residue), cleaved process catalyzed exclusively by ZMPSTE24, leading to the release of the mature lamin A protein (a 664 amino acids peptide) (Figure 5). In a recent publication, Dumont's group investigated the structure and catalytic cleavage of a-factor by the year Ste24p enzyme and compared it to the mechanism of the same step for prelamin A. [10]

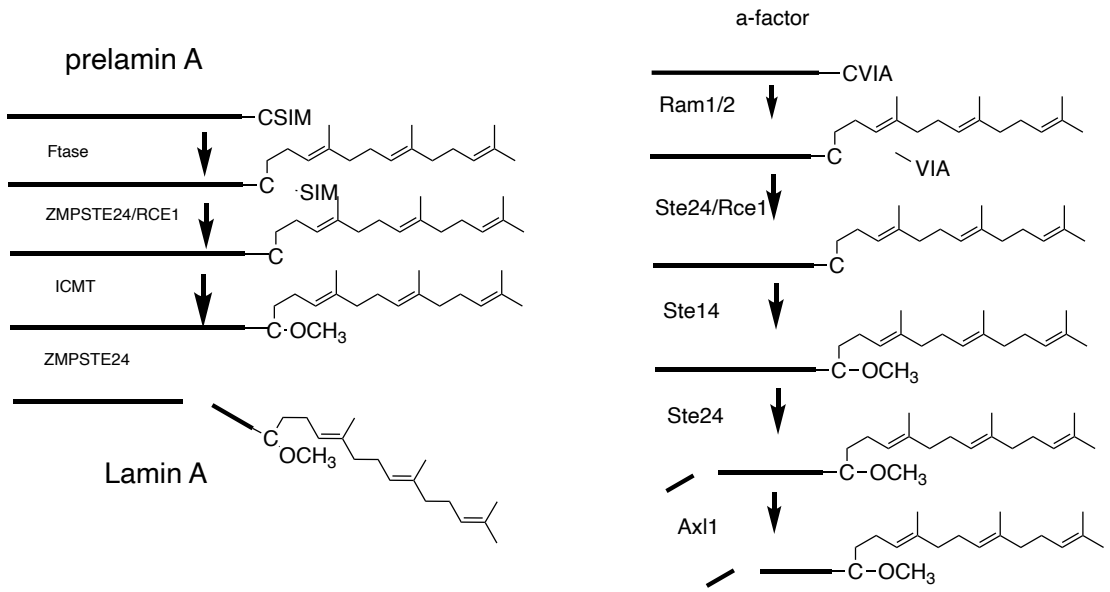

Figure 5. The processing of cleavage for lamin A and a- factor. (**A**) The maturation pathway for lamin A in human cells. Prelamin A is a protein which length in 74 kDa, its C-terminus has a CSIM motif. (**B**) The maturation pathway for a-factor in yeast cells. The a-factor is length in 1.6 kDa, and CVIA motif is located the C- terminus which triggers the CaaX processing.

Recent biochemical studies strongly suggest that ZMPSTE24 may be a valuable therapeutic target for cancer treatment, due to its association with cell migration (metastasis) and proliferation. [41] Although potent and selective inhibitors of ZMPSTE24 have not been reported yet, some HIV protease inhibitors have been found to exhibit weak activity in inhibiting ZMPSTE24; the structure and IC_{50} value of the HIV protease inhibitors will be discussed in a later section. [42] Nowadays new chemical compounds are synthesized to inhibit the migration of tumor cells, and they may also reduce DNA damage. Furthermore, Dorf's group has proposed that ZMPSTE24 is a broad-spectrum antiviral factor in our body that can prevent the invasion of DNA and RNA viruses. [43]

1.6. Structure of ZMPSTE24

The structure of ZMPSTE24 contains seven transmembrane helices and a cytoplastic cap (Fig. 6A). [40] These elements construct a barrel-like structure, which involves an extremely large internal cavity (that can accommodate a 10 kDa protein or 1,000 water molecules) and contains a Zn^{2+}

cation. [44] The zinc ion is surrounded and coordinated by a cluster of HEXXH residues within the active site (Fig. 6B). The seven transmembrane helices are assembled into an antiparallel α-helical bundle. [45] The whole structure is most stable when the chamber is filled with water. Based on X-ray crystallographic data, the structure of ZMPSTE24 has been shown to be very similar to Ste24p and its active site resembles that of thermolysin. [40]

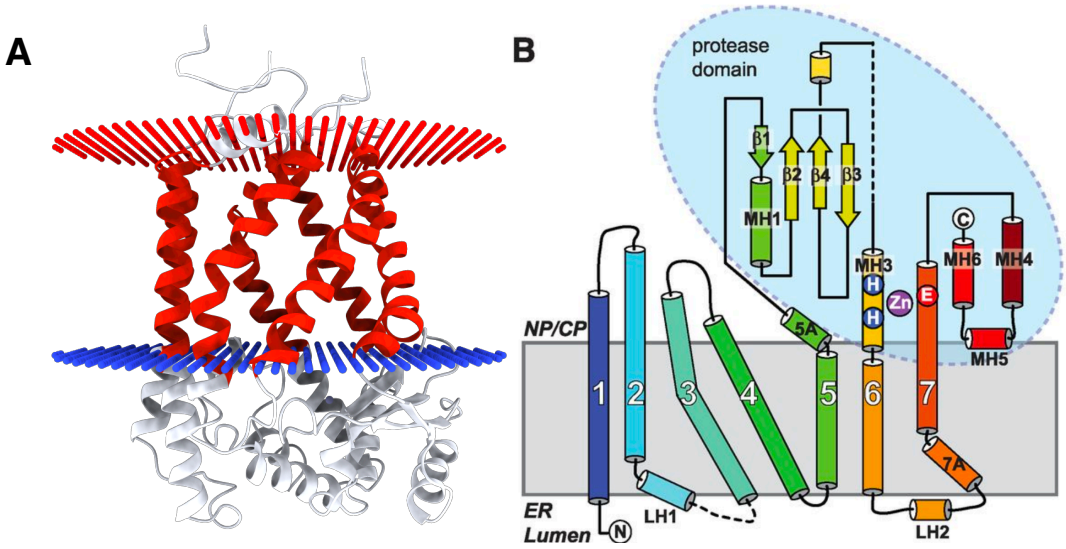

Figure 6. Crystal structure of ZMPSTE24 [PDB ID 4AW6]. (**A**) The 3D model shows the structure of ZMPSTE24. Seven helices are colored in red. (**B**) Topology diagram highlighting the arrangement of TMHs, the structure is colored from blue to red from N to C terminus. The metalloprotease fold is highlighted in pale blue. [25]

The seven transmembrane helices of the ZMPSTE24 structure [41] are named as helix I to VII, based on the similarity of this enzyme with the structure of Ste24p. [10] There are significant curves present between helices III to VII, and helix VI contains the Zn^{2+}-dependent active site within its HEXXH motif. Two luminal loops, between helices II and III and between helices VI and VII, contain short helices in these two parts respectively. [45] There are two additional domains which block big gaps between helices V and VI and between helices VII and I: loop 5 domain (L5D) and C- terminal domain (CTD). In a recent report, Dumont's group showed that there is a larger

opening on L5D domain for the efficient entry or egress of the substrate the active site of the enzyme (Fig. 7B). [40] This gap can also provide a channel for the farnesyl moiety on the farnesylated substrate to penetrate through the protein.

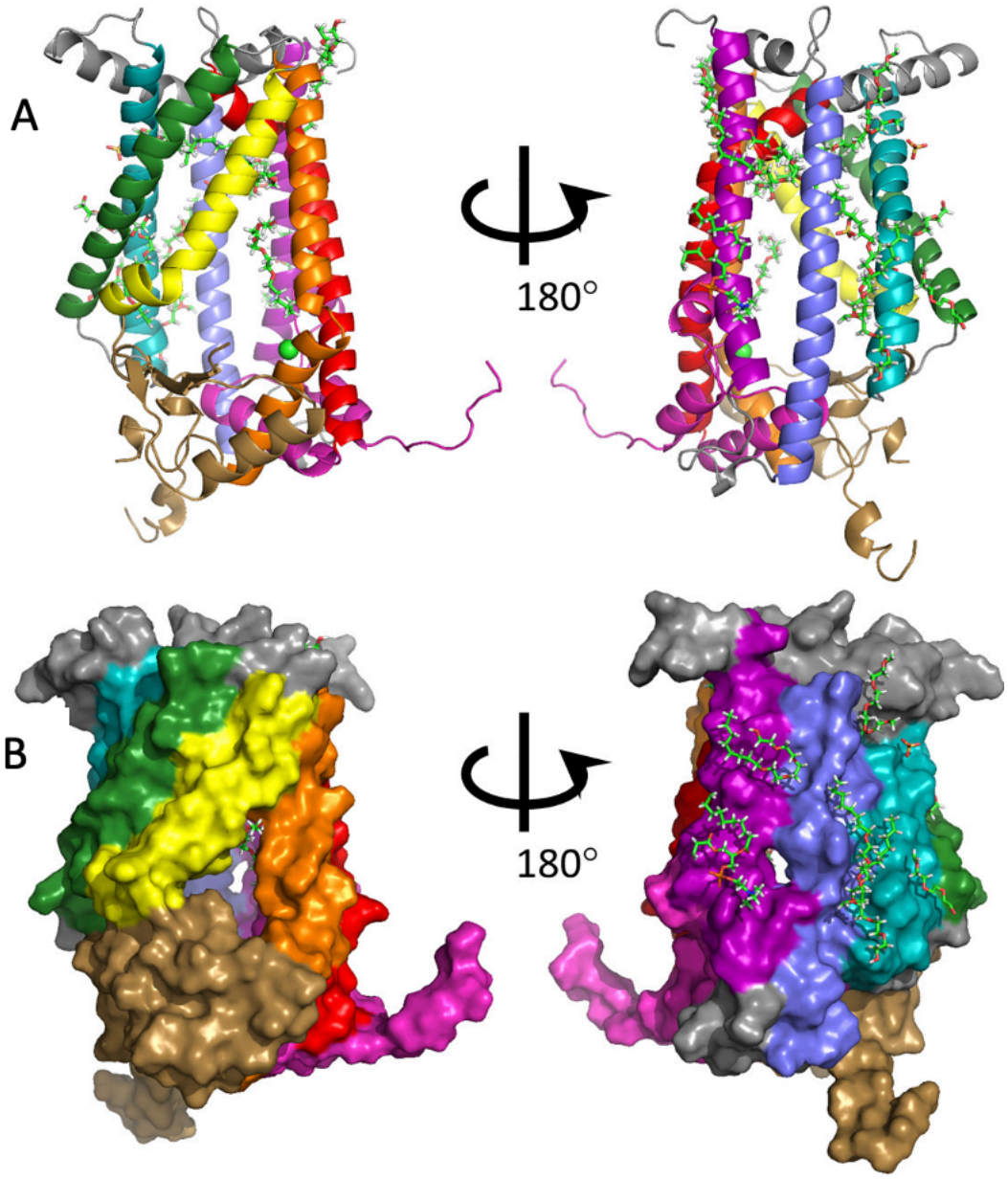

Figure 7. Overall structure of ZMPSTE24. [40] The angles of view and coloring of secondary structure elements are as presented for yeast SmSte24p. Helix I, purple; helix 2, blue; helix 3, cyan; helix IV, green, helix V, yellow, helix Vi, orange; helix VII, red; cytosolic loop 5 domain, brown,

C-terminus, pink. (**A**) Cartoon view. (**B**) Surface representation. The zinc ion is shown in light green. Presumed lipid, sulfate, and polyethylene glycol or detergent molecules are shown in stick representations.

The water in the internal cavity of the enzyme plays an important role for the whole structure and function of ZMPSTE24. Two molecules of water which are closest to the Zn^{2+} ion may suggest a new pathway in the catalytic mechanism, as consumption of multiple water molecules occurs during the hydrolysis reaction. These two molecules water interact with the Zn^{2+} ion and they form a tetrahedral arrangement, along with three amino acids around the zinc. The active site of ZMPSTE24 envelops the zinc ion coordinated by H335 and H339 in the HEXXH motif and E415 from helix VII, which is similar to the active site of thermolysin (Figure 8). The catalytic residue is E336 of the HEXXH motif, participating in water coordination for initiating the nucleophilic attack. The electrostatic surfaces in the interior of cavity of ZMPSTE24 are negatively charged which could cause a favorable interaction with the zinc ion. [40] Similar to other zinc metalloproteases, the highly conserved hydrophobic residues that are present in S1' and S2' sites are considered to be related to substrate specificity.

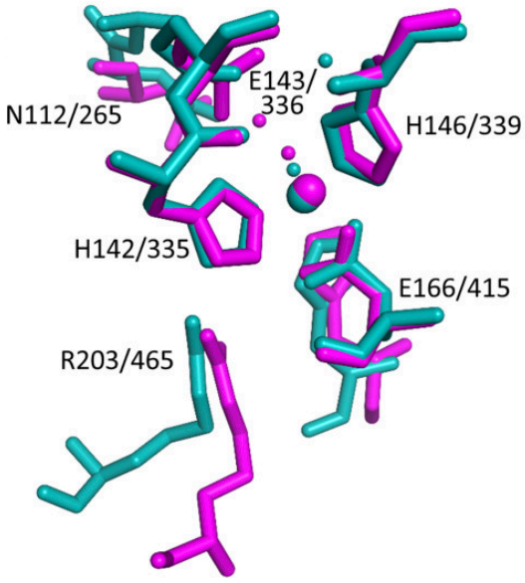

Figure 8. ZMPSTE24 active site. [40] The view of a comparison of the active sites of thermolysin (PDB: 8TLN) and ZMPSTE24. Atoms from thermolysin are shown in cyan, atoms

from ZMPSTE24 are shown in magenta. Labels indicate the position of the indicated residues in thermolysin/ZMPSTE24). Zinc is shown as a large sphere. Water molecules closes to the zinc are shown as small balls with appropriate coloring. The positions of eight residues from thermolysin that were previously found to adopt similar positions in yeast Ste24p17 are indicated. Only seven of these positions are found in the ordered regions of ZMPSTE24.

1.7. Catalytic Mechanism

The catalytic mechanism of ZMPSTE24 is a two-step process (Figure. 6A). In the first step, the prelamin A enters the cavity and binds to the zinc ion, which forms a five-coordinated transition state (Figure. 6A). In the second step, the carbonyl of the amide bond is attacked by the nucleophilic water molecule. One of the hydrogen atoms is transferred from the water molecule to E336 (Figure. 6A). Then, the catalytic ligand E336 forms a hydrogen bonding to a water molecule and the position of this residue changes significantly after substrate binding (Fig. 9A). Some conserved residues, such as N265, H459 and R465 play a role in the stabilization of transition state by forming hydrogen bonding with the peptide substrate (Fig. 9B).

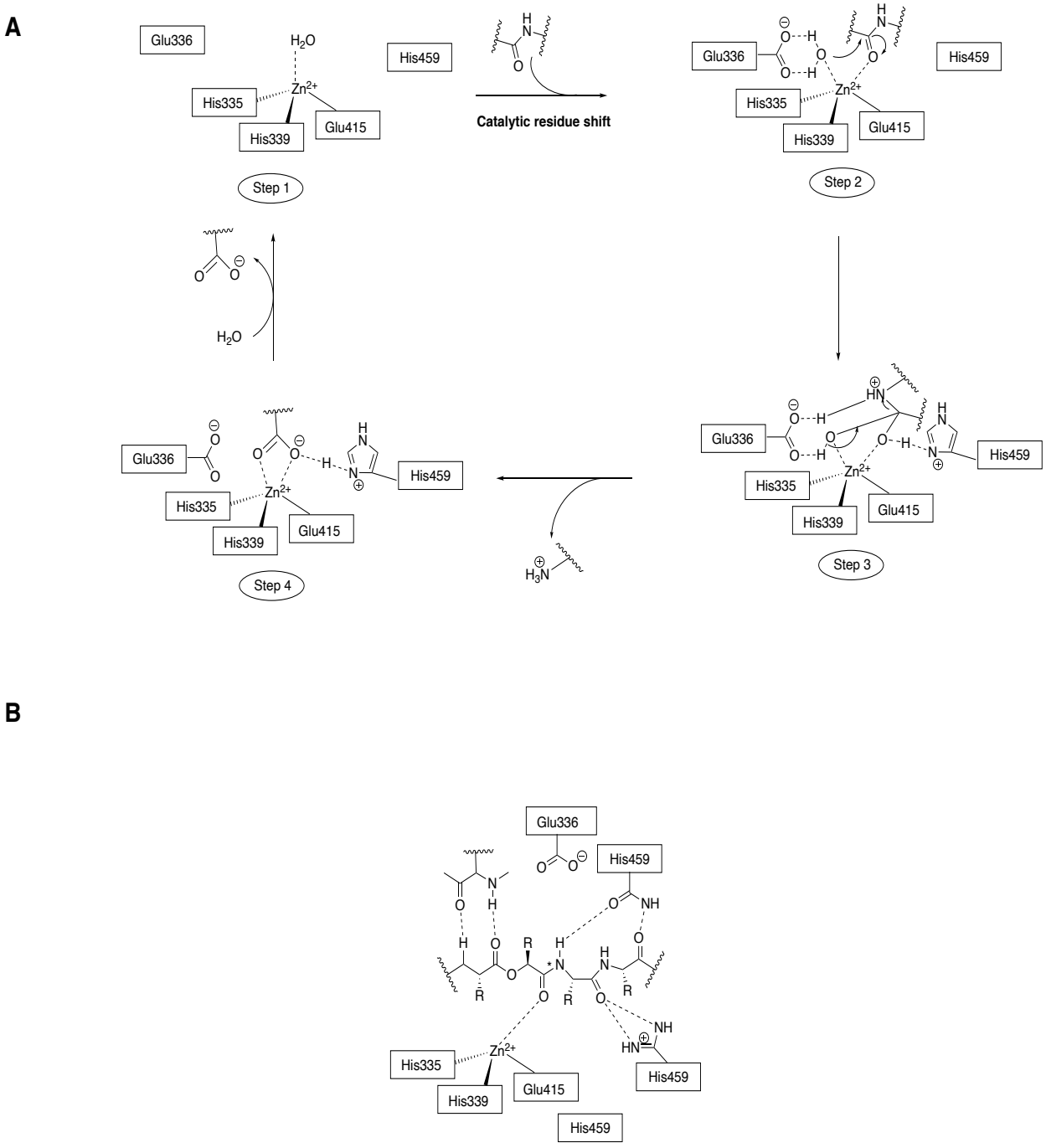

Figure 9. Proposed catalytic. mechanism for ZMPSTE24. [45] (**A**) Reaction mechanism based on the generally accepted two-step mechanism of peptide hydrolysis by thermolysin.**Error! Bookmark not defined.**,**Error! Bookmark not defined.** The scissile amide bond of the substrate is represented. (**B**) Schematic representation of peptide binding to the active site of ZMPSTE24. Residues coordinating the catalytic zinc ion and residues that interact with the substrate are shown in boxes. Circles refer to the standard peptide subsite positions relative to the scissile bond.

1.8. The effect of accumulation of prelamin A in human diseases

Lamin A is one of the lamin filaments that constitutes the structural component of the nuclear lumina, and it plays an important role in the nuclear morphology and the stability of the nuclear scaffold, gene expression, mitosis, DNA replication, and cell proliferation. The lack of lamin A gene, LMNA, causes the abnormal morphology of nuclear (multinucleation) and DNA damage response (DDR), which reflects on the mitosis arrests, and shorten telomere. [46] The process leading to lamin A maturation is quite important for maintaining the cell's basic structure and function. Zmpste24 and LMNA deficiencies lead to profound nuclear architecture abnormalities and multiple histopathological defects that accelerated the ageing process. [47] Bergo's group reported muscle weakness and bone fractures in ZMPSTE24 deficient mice, they suggested the "muscle weakness" syndrome was due to the downregulation of prelamin A processing. [48] Mutations in the prelamin A sequence that can block the catalytic function of ZMPSTE24 and consequently, the maturation of lamin A, leading to major phenotypic changes in various mesenchymal tissues. [49] Similarly, Bonne's group noticed that mutation of LMNA gene, which encodes the prelamin A/lamin C proteins, can cause the Emery-Dreifuss muscular dystrophy (EDMD), [50] Dunnigan-type familial partial lipodystrophy (FPLD), [51] limb-girdle muscular dystrophy and EDMD, which are attributed to the accumulation of prelamin A. In addition, mandibuloacral dysplasia, restrictive dermopathy and progeria are also known to be caused by lamin A maturation defects. [49, 52, 53]

Progeria, which also called as Hutchinson-Gilford progeria syndrome (HGPS), is a rare and fatal "premature aging" disease. [54] Most of the children die from progressive cardiovascular abnormalities in progeria before age of 13. [49, 55] The high amounts of farnesylated prelamin A accumulation is the main reason for the HGPS syndrome in children. [47,56] Cells that express progerin have genomic instability, telomere disorder, altered histone genetic modification, chromosome segregation and mutants in nuclear architecture. The inhibition of ZMPSTE24 activity can cause nuclear architecture abnormalities, a shortened lifespan and ageing associated phenotypes. Similarly, ZMPSTE24 deficiency or inhibition of its catalytic activity cause prelamin A accumulation in cells and activation of the p53 pathway. [46]

The p53 factor is a transcription factor which plays an important role in the cell cycle and acts as an important tumor suppressor. [57] The p53 pathway is part of the cell senescence or apoptosis

mechanism which prevents the invasion of healthy tissues by tumor cells. In a ZMPSTE24 deficient animal model, the level of p53 target genes (such as p21, Gadd45a and Rtp801) were upregulated which reflects the relations between the activation of p53 stress response pathway and the mutants in the processing of lamin A maturation. [47] The p53 pathway also limits DNA replication, DNA damage and multinucleation of cells, thus participates in the process of maintaining normal cell morphology and replication. [56]

Interestingly, the accumulation of prelamin A in cells and the rewiring of extracellular matrix (ECM)-related cellular pathway also cause significant decrease of cancer cell's invasive potential. In 2013, López-Otín's group established a "mosaic" rat model which can keep similar proportions of ZMPSTE24-deficient (prelamin A-accumulating) and normal cells in order to study the relationship between extracellular matrix (ECM) and progeria pathogenesis. [41] In previous research, they found that ECM and its related factors are the major factors influencing cancer invasion. [60] The accumulation of prelamin A can led to deficient DNA replicative capacity through ECM-mediated mechanisms. [41] Also, the progeria markers, such as the expression level of p53-target genes (Cdkn1a, Igfbp3 and Atf3) reflect that cell-extrinsic mechanisms are preeminent in the onset and development of prelamin A-induced progeria. In this research, their group showed that the accumulation of prelamin A does not affect tumor initiation but prevents cancer invasion (a biological procees requirted for cancer metastasis), which suggests that ZMPSTE24 may be a valuable therapeutic target for the treatment of cancer. [41, 46] It should be noted that of the impact of permenent prelamin A accumulation, as in the case of HGPS, is very different from the temporary and only partial decrease in prelamin A processing during cancer therapy.

1.9. Inhibitors of ZMPSTE24

The human immunodeficiency viruse (HIV) is a retroviruse responsible from acquired immunodeficiency syndrome (AIDS). HIV protease inhibitors (HIV PIs) combined with many other antivirals, such as polymerase, integrase and entry inhibitors are used to supress HIV replication *in vivo*. [61] HIV protease is an aspartyl protease, which has a similar mechanism of action as zinc metalloproteases, in that both types of enzymes use a nucleophilic water molecule to facilitate the hydrolytic cleavage of amide bonds. [62] Recently, Young's and Dumont's groups reported that some HIV PIs can weakly inhibit the enzymatic activity of Ste24p and ZMPSTE24,

and they suggested this off-target effect may be the reason for highly active antiretroviral therapy (HAART) resulting in the accumulation of prelamin A. [40, 44, 63, 64] Various HIV PIs have different affinities for ZMPSTE24, and the inhibition might be the result due to the factors such as solubility and affinity, because inhibitors do not appear to be bound in any well-ordered configuration in the crystals. [40] Using native mass spectrometry studies, Robinson's group confirmed that lopinavir has a higher affinity for ZMPSTE24 than ritonavir, with Kd values of approximately 25 μM and 30 μM, respectively (Fig. 10). [44] Dumont's group also reported that the IC_{50} value of lopinavir (IC_{50} ~ 18 μM) [58] is lower than other HIV PIs such as atazanavir and ritonavir. [40]

Efforts in our own research group, [62] have identified several small-molecule inhibitors that block lamin A maturation, leading to intracellular accumulation of prelamin A and arrest of cancer cell migration; a biological effect that is required for cancer cell metastasis. Example of the compounds (compound **1** and **2**) identified are shown in the figure below (Figure 10).

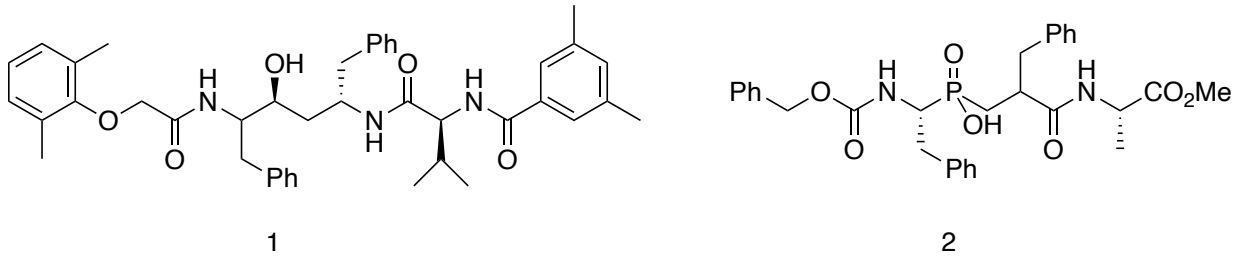

Figure 10. Chemical structure of ZMPSTE24 inhibitors 1 and 2. [62] Two compounds are selected from a library of compounds. Peptidomimetic analogs **1** and **2** are more potent in blocking prelamin A processing than the HIV PI lopinavir. Compound **2** showed higher potency than **1** and inhibited cancer cell migration.

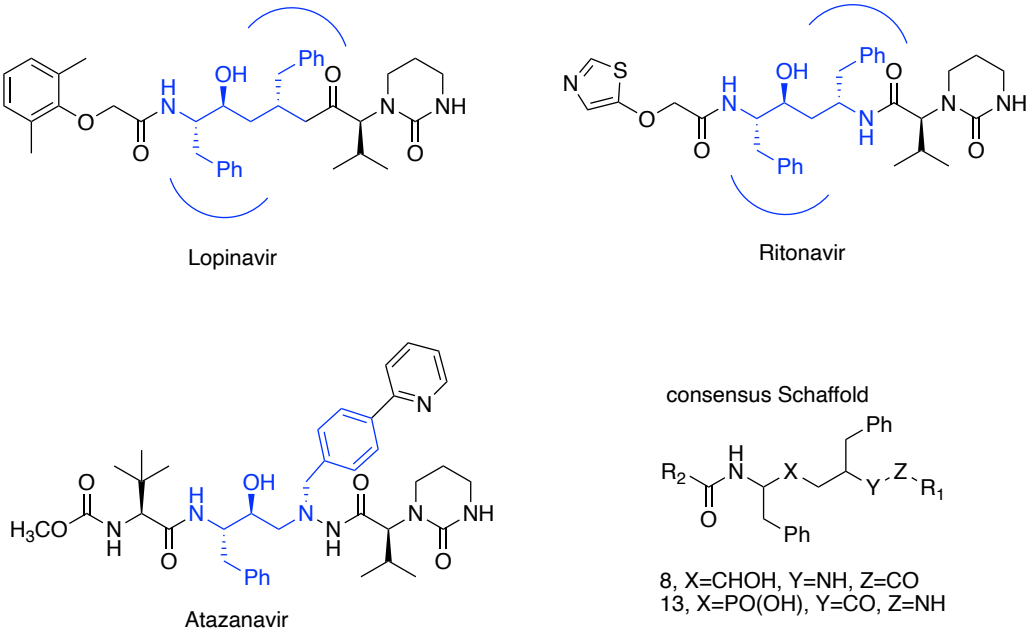

Figure 11. Structure of HIV PIs and consensus Scaffold. The minimal consensus scaffold (1&2) is based on the basic structure of HIV PIs. The blue part means the key transition-state mimics. [62]

The mevalonate pathway is relevant to the synthesis of isoprenoids, such as farnesyl pyrophosphate, which the substrate required for the farnesylation of prelamin A. [66] Two enzymes in the mevalonate pathway, hydroxymethylglutaryl coenzyme A (HMG-CoA) reductase and farnesyl pyrophosphate synthase (hFPPS), [62] have been targeted with statins (e.g. pravastatin) or nitrogen containing bisphosphonate drugs (e.g. zoledronic acid), in order to block farnesylation of prelamin A [66] Other enzyme inhibitors in that also affect the processing of prelamin A include the farnesyl transferase enzyme (FT) that can block the farnesylation step and consequently, lead to the accumulation of nonfarnesylated prelamin A; these compounds have been used to reduce the syndrome of HGPS. [44] Experimental evidence also suggests that rapamycin can decrease DNA damage and can restore chromosome positioning in the interphase of HGPS nuclei which affect the cell's ability to regulate proper genome function. [67, 68]

Peptidomimetic inhibitors are usually active site inhibitors of protease enzymes that mimic the natural substrates but are inert to the enzymatic cleavage. Compared to the peptide bonds of natural substrates, several different modifications are made to amino acids or peptide bonds, including carbonyl substitution, N- or Cα substitutions, incorporation of unnatural amino acids and

backbone extension. The goal of my MSc research was the expression, isolation and purification of the human recombinant ZMPSTE24 protein that can be used in our medicinal chemistry studies to evaluate the potency of our novel ZMPSTE24 inhibitors and their mode of binding to this enzyme by MS and X-ray crystallography.

2. Experimental, Research Findings and Discussion

2.1. Growth of yeast for ZMPSTE24 expression

We are grateful to Professor Mark E. Dumont (Department of Biochemistry and Biophysics; University of Rochester) for a generous gift of the yeast strain YO1362 that overexpresses the human recombinant ZMPSTE24 enzyme. This strain of *S. cerevisiae* expresses the enzyme under the control of the ADH2 promoter as a C-terminal fusion and contains a cleavable ZZ-His10 tag. The ADH2 promoter (P(ADH2)) is repressed several hundred-fold in the presence of glucose; transcription is initiated once the glucose in the medium is exhausted. [69] For ZZ peptide-tag, "Z" means Z domain, which is a synthetic IgG-binding protein. This domain is derived from the B domain of staphylococcal Protein A. The resulting human ZMPSTE24 protein could be expressed in large amounts, allowing purification of 10 mg of crude membrane which contained ZMPSTE24 from 9 liters of cell culture.

Yeast YO1362 strain was first cultured in 100 mL mini-culture rich media. After one day of cell proliferation, the yeast cells were transferred and cultivated in selective media (SD-ura, synthetic defined yeast medium, without uracil) to selectively grow yeast cells. Then the cells were cultivated in a 9 Litter BioFlo 3000 fermenter for reproduction and overexpression. The cells were proliferated for 24 h until the glucose in the medium was fully depleted (Fig. 12), and subsequently, the culture allowed to produce the ZMPSTE24 protein for an additional 24 h.

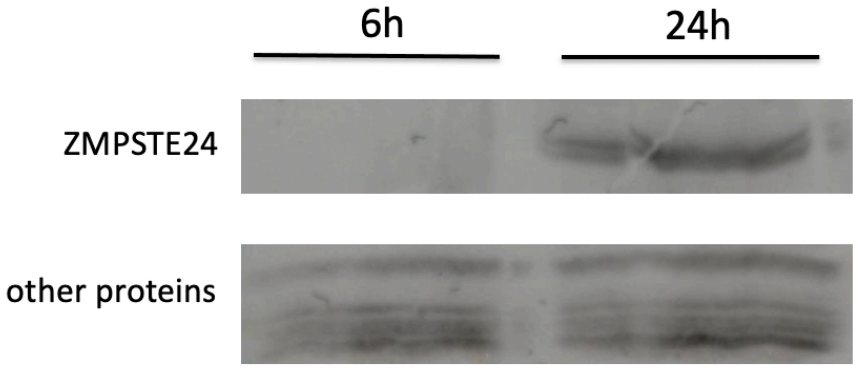

Figure 12. SDS PAGE gel indicating the expression of human ZMPSTE24. The yeast strain YO1362 is cultivated in BioFlo 3000 for 24 h until the glucose in medium is depleted and the ZMPSTE24 protein begins to be expressed in yeast cells. The samples were collected in 6 h and 24 h post glucose depletion. The concentration of the ZMPSTE24 at 24-hour is much higher than at 6-hour post glucose depletion in the yeast culture.

2.2. Cell lysis and purification

2.2.1. Cell lysis

The ZMPSTE24 protein is fused to a His-tag, which can bind to the anti-His primary antibody and identified by Western Blot analysis. The cells were lysed by homogenizing them using an Avestin C5 homogenizer, and the transmembrane proteins were solubilized in lysis buffer by adding n-dodecyl-β-maltoside (DDM) detergent. DDM is often the first choice of detergent for solubilizing membrane-bound proteins due to its rather mild denaturation properties.

2.2.2. Protein affinity chromatography

In addition to the His-tag, the ZMPSTE24 enzyme is expressed as a fused protein with a ZZ peptide-tag that can bind to an IgG resin (i.e., a solid support with an immobilized antibody for the ZZ peptide attached to the resin) and consequently, purified by affinity chromatography. ZZ-tag is consisted of 58 amino acids and its length is 18 kDa. [70] The IgG resin was incubated with the DDM solution of the ZMPSTE24-ZZ-His_{10}-tag protein overnight at 4°C in order to fully adsorb the protein onto the resin. After ZMPSTE24 adsorption steps, the IgG resin was incubated with

the human rhinovirus 3C protease (HRV-3C) for 2 h, in order to cleave the His_{10}-tag located at the C-terminal of the ZMPSTE24 protein and the ZZ-tag. After the cleavage steps, the ZMPSTE24 solution is incubated with nickel affinity resin to remove the HRV-3C protease which contained His6-tag in solution.

The samples are collected after each steps of the above purification experiments. In the initial Western Blot assay for the isolation of the crude ZMPSET24-ZZ-His_{10} protein construct, the primary antibody that was used was an anti-His antibody that binds to fuse His-tag. However, in this second stage of purification a specific anti-ZMPSTE24 primary antibody was used to selectively bind to ZMPSTE24 protein (Fig. 13B). The band of denatured ZMPSTE24 is reflected on SDS PAGE gel after changing the primary antibody during the Western Blot analysis (Figure 13).

The transmembrane protein, ZMPSTE24, is congested on the gel well, and the protein cannot run on the gel due to the denaturation and protein aggradation. The results of aggradation may be caused by the heating steps (heat ZMPSTE24 at 95°C to denature protein), because the transmembrane protein is significantly unstable under the heating steps or even at room temperature.

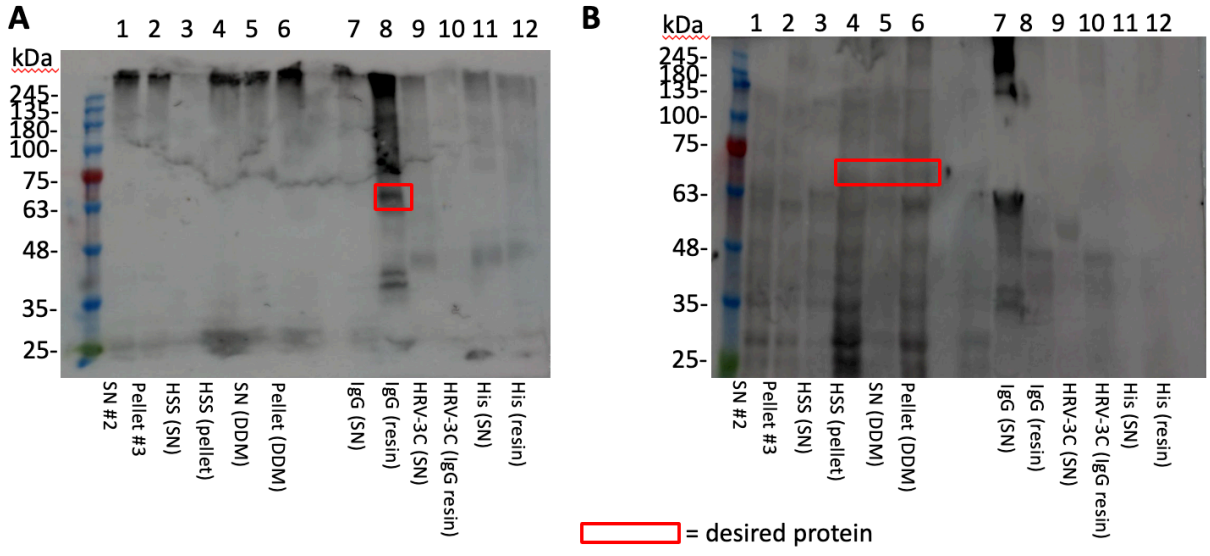

Figure 13. Samples collected from cell lysis steps. The samples are reflected on SDS PAGE gel and analyzed by Western Blot. The desired protein is the ZZ-His10 tagged ZMPSTE24. (**A**) The samples are collected from each cell lysis steps, and the protein ZMPSTE24 is specifically bind to anti-ZMPSTE24 antibody and show bands on Western Blot gel. SN #2, the supernatant collected the second homogenizing step; Pellet #3, the pellets collected after centrifuging steps; HSS (SN), the supernatant collected from ultracentrifuge (HSS, high speed spin); HSS (pellet), the pellets collected from HSS; Pellet (DDM), the pellets collected after adding DDM in protein solution; IgG (SN), the supernatant collected after IgG incubation step; IgG (resin), the resin sample from the IgG incubation step; HRV-3C (SN), the supernatant collected after cleavage steps; HRV-3C (IgG resin), the IgG resin collected after cleavage steps; His (SN), the supernatant collected after ICMT steps; His (resin), the resin collected after ICMT steps. (**B**) The samples are collected from each cell lysis steps, and the protein ZMPSTE24 is shown to specifically bind to anti-ZMPSTE24 antibody by Western Blot analysis.

2.2.3. Size elution chromatography

After the affinity purification steps, the sample solution was purified by size expulsing chromatography on a Superdex 200 column All fractions were using an FPLC instrument (Fig. 14A).

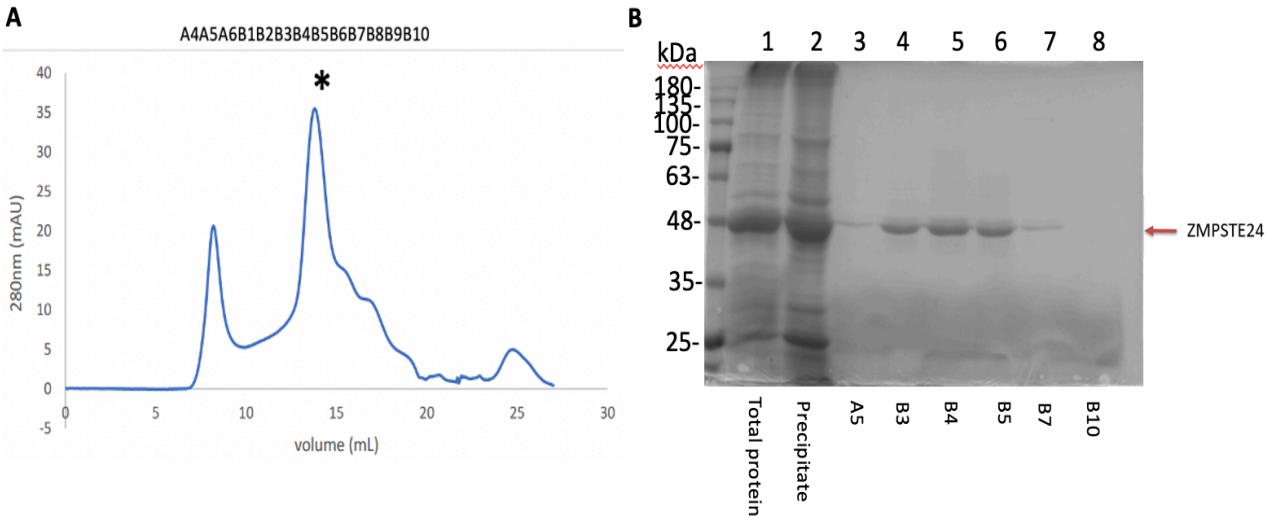

Figure 14. Elution chromatogram of ZMPSTE24 by sizer exclusion chromatography and SDS gel of fractions. (**A**) The fraction curve of ZMPSTE24 after elution steps by size elution chromatography. *The fraction peak of ZMPSTE24. (**B**) The SDS gel of protein fraction from size elution chromatography. Total protein: the sample solution is the combination of fraction B3 ~ B7; Precipitate: the sample is collected after total protein sample concentration; A5, B3 ~ B10: The samples collected from size elution chromatography.

The protein ZMPSTE24 was eluted using a polyoxymethylene detergent $C_{12}E_7$. The fraction curve shows two protein peaks (Figure. 11, A), which likely reflects some aggravated proteins (fraction A4 ~ A6, 115 kDa) and ZMPSTE24 (fraction B3 ~ B10). It is noteworthy that although the molecular weight of ZMPSTE24 is approximately 54kDa, it has been reported by Dumont and others to migrate at approximately 48-50 kDa, as shown in Figure 14B. The identity of the major band shown in Figure 14B (fractions B3-5) was further confirmed to be ZMPSTE24 by in-gel digestion, followed by MALDI-MS analysis. The fractions of the ZMPSTE24 protein were collected, concentrated to 10 aliquots and stored at -80^{o}C to be used in future studies.

2.3. Mass Spectrometry

2.3.1. MALDI analysis

An aliquot of the ZMPSTE24 protein was transferred from -80°C to 4°C. After the gel filtration chromatography, the sample should be analyzed by MALDI analysis immediately to prevent the denaturation of protein. MALDI is a soft ionization method which involves a laser hitting a small molecule matrix so that the analyte molecules enter the gas phase without breaking or decomposing. The protein solution was filtered through C18 desalting column. The column is pre-equilibrated by ACN and TFA solution. After the desalting preparation, the protein solution was mixed with DHB matrix on a polished steel target and analyzed in linear-positive ionization mode, the MALDI data shows the target protein in the sample (Figure 15).

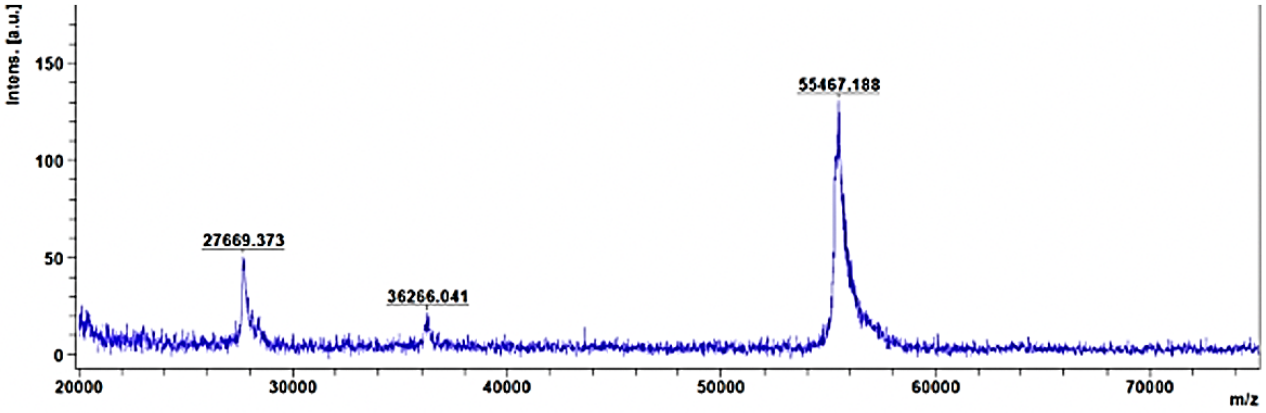

Figure 15. Preliminary MALDI result data for human ZMPSTE24 protein. The spectrum for intact ZMPSTE24 matches anticipated peaks at m/z of 27,771 $[M + 2H]^{2+}$ and 55,542 $[M + H]^{+}$. Standards or samples were spotted 1:1 with DHB matrix on a polished steel target and analyzed in linear-positive ionization mode (500 shots × 4 = 2,000 shots total per sample). Modest differences between the measured and theoretical average masses are due to the linear detection mode used.

In the above MALDI analysis, bovine serum albumin (BSA; MW 66.4 kDa) and Protein A (MW 44.6 kDa) were chosen as standard samples to ensure the accuracy of calibration and our results. The spectrum for protein A at 22,307 $[M+2H]^{2+}$ and 44,613 $[M+H]^{+}$ m/z (mass to charge ratio), as well as BSA at 33,216 $[M+2H]^{2+}$ and 66,432 $[M+H]^{+}$ m/z. The MALDI spectrum for protein ZMPSTE24 matches peaks at 27,771 $[M + 2H]^{2+}$ and 55,542 $[M + H]^{+}$ m/z. The peak of ZMPSTE24 is around 50 Da off from the predicted mass of around 55,579 Da (from Robinson paper). [44] In summary, the MALDI analysis confirmed that the isolated protein corresponds to the molecular weight of ZMPSTE24

2.3.2. Efforts Towards Detection of ZMPSTE24 by Native Mass Spectrometry

After the protein purification steps and the MALDI analysis, efforts were made to also confirm the identity of ZMPSTE24 by native MS analysis, as previously reported, [44] Native MS is a method that allows testing of the large biomolecules and non-covalent complexes of such

biomolecules, for example it allows detection of inhibitors bound to an enzyme. A aliquot of the purified ZMPSTE24 protein was transferred from -80°C to 4°C, and the buffer was exchanged with MS buffer containing ammonium acetate and C8E4 detergent. The protein was diluted in the MS buffer, however, based on previous reports, this technique requires high concentrations of protein (at least 15 μM) in order to be successful. Unfortunately, in our case, the concentration was much lower, and no meaningful signal could be observed (Fig. 16B); the reasons for the loss of native protein are currently unclear, however, given the physiological properties of this enzyme, it is likely that the protein precipitates out of solution during concentration. It is noteworthy that in the original paper by Robinson's group, [44] both the apo ZMPSTE24 enzyme (with and without a bound Zn^{2+} ion) was characterized by this technique, as well as such as the ZMPSTE24-lopinavir complex. The molecular weight of ZMPSTE24 is around 55 kDa with charges of 11 plus. The anticipated human ZMPSTE24 peak should be confirmed at around 3,500 m/z. However, in our case the result for the protein sample did not show the corresponding mass between 3,500-5,000 m/z (Fig. 16A). In the future, re-purification of this enzyme and more careful evaluation of the sample preparation for MS should allow us to reproduce these results.

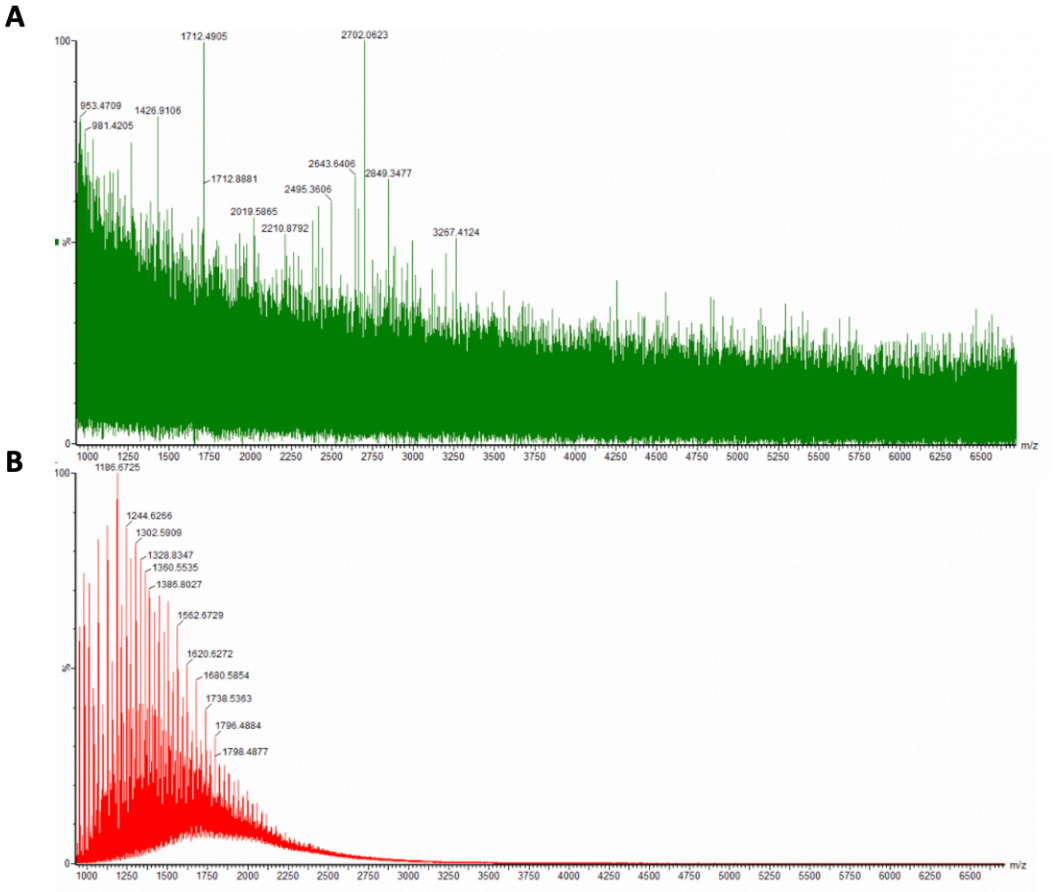

Figure 16. Native Mass spectrometry result data for human ZMPSTE24 protein. (**A**) The native MS result data for human ZMPSTE24 protein after the buffer exchange steps. (**B**) The native MS result data for 6 aliquots of samples without the buffer exchange steps.

2.4. Conclusion and Future directions

2.4.1. Conclusion

The human ZMPSTE24 protein is a membrane-bound zinc metalloprotease. ZMPSTE24 is essential for the maturation of the filament protein lamin A from its precursor protein prelamin A. The filament proteins lamin A and lamin C are essential structural proteins of the nuclear lumina. The inhibition of ZMPSTE24 has been shown to have significant effects on the shape of nuclei morphology and cell mitosis. The protein of ZMPSTE24 was expressed as a construct of the fused peptide ZMPSTE24-ZZ-His_{10} in the yeast strain YO1362 (generously donated by Prof. Mark Dumont) and the crude membrane-bound enzyme was purified by affinity chromatography using

IgG resin and ICMT affinity chromatography. After two purification steps, the sample fractions were further purified by size elution chromatography. MALDI MS analysis confirmed that the isolated protein was the same molecular weight as ZMPSTE24, however, due to low concentration of the detergent solubilized enzyme at the last step of purification, detection of ZMPSTE24 by native MS analysis was not successful.

2.4.2. Further Directions

Although we were successful in the expression and purification of the human ZMPSTE24 enzyme from yeast and confirmed its purity by Wester Blots and the MALDI MS analysis, the concentration of the final enzyme solution was not sufficient for successful characterization by native MS. Membrane-bound proteins present a significant challenge in their purification, as they can easily precipitate or aggregate in solution, and the solutions must contain a large amount of detergent. Our future plans are to re-express and purify larger quantities of this enzyme in order to (a) use it to develop an in vitro FRET-based inhibition assay and evaluate bind of our ZMPSTE24 inhibitors by native MS.

Additionally, large amounts of protein will also allow crystallographic experiments in the presence of bound inhibitors that can guide our medicinal chemistry efforts. Co-crystal structure of ZMPSTE24-inhibitor complexes are not currently available at high resolution; such structures can reveal the binding mode of inhibitors and guide SAR studies.

3.Materials and Methods

3.1 Equipment

- Pipettes (10, 100, 1000 ul)
- VWR® Chromatography Refrigerators with Glass Doors and Natural Refrigerant, Basic
- Western Blotting (Bio-Rad: PowerPac™ HC High-Current Power Supply, Mini Trans-Blot® Cell. ImageQuant LAS 500 chemiluminescence CCD camera)
- Flasks (200 mL, 2 L, 4 L)
- Avestin Emulsiflex C5 Homogenizer
- Waters Syanpt G2 - Si (Q-TOF)
- Centrifuge (1.5 ml, 15 ml, 50 ml, 500 ml), ultracentrifuge
- ÄKTA go goes even more compact – NEW dual plate fraction collector F9
- HiLoad® 16/600 Superdex® 200 pg (GE Healthcare, 120 mL bed volume)
- pH Sensor 405-DPAS-SC-K8S/325
- BioFlo3000 fermenter (New Brunswick Scientific)
- Incubating orbital shaker, Orbital shaker
- Blood glucose monitor
- Cellulose centrifugal concentrator (Millipore)
- Roller-Mixer
- Spin desalting column
- NanoDrop™ 3300 Fluorospectrometer (Thermo Fisher Scientific)
- MSP 96 target polished steel BC (Bruker, Cat. # 8280800)
- MALDI UltrafleXtreme® system (Bruker)
- Pierce™ C18 Spin Columns (Thermo Scientific, Cat. # 89873)
- Micro Bio-Spin™ Chromatography Columns (Bio-Rad, Cat. # 7326204)

3.2 Reagents

- Clarity Western ECL Substrate (Cat. #1705061)
- Heptaethyleneglycol mono n-dodecyl ether ($C_{12}E_7$ detergent), tetraethylene glycol monooctyl ether (C_8E_4 detergent) and n-dodecyl-β-maltoside (DDM detergent)
- Lysis Buffer: 20 mM Hepes pH 7.5, 150 mM NaCl, 15% (w/v) glycerol ~ 12% (v/v), 1 mM DTT (add prior to use), 100 uM PMSF (add prior to use).
- Wash Buffer: 20mM Hepes pH 7.5, 150 mM NaCl, 15% (w/v) glycerol ~ 12% (v/v), 1mM DTT (add prior to use), 100 uM PMSF (add prior to use), 0.04% $C_{12}E_7$.
- IgG Binding Buffer: 20 mM Hepes pH 7.5, 150 mM NaCl, 15% (w/v) glycerol ~ 12% (v/v), 0.01% (w/v) DDM (add prior to use).
- Gel Filtration Buffer: 20 mM Hepes pH 7.5, 150 mM NaCl, 5% (w/v) glycerol ~ 4% (v/v), 1 mM DTT (add prior to use), 0.04% $C_{12}E_7$.
- Mass spectrometry Buffer: 200 mM ammonium acetate, 0.5% C_8E_4.
- HRV-3C Protease (human rhinovirus 3C protease, N-Terminal His tagged recombinant protein) (Sigma Aldrich, Cat. #SAE0045)
- IgG Sepharose 6 Fast Flow Affinity Resin (GE Healthcare, Cat. # 17096901)
- cOmplete™ His-Tag Purification Column (Roche, Cat. # 6781535001)
- 2,5-Dihydroxybenzoic acid (DHB) (Cat. # 85707)

3.3 Cell Culture, Protein expression and purification

3.3.1 Yeast strain

All the yeast stains were obtained from Dumont group. The human ZMPSTE24 was expressed in baker's yeast *Saccharomyces cerevisiae*. The gene of ZMPSTE24 is under control of the ADH2 promoter and is fused to C-terminal IgG-binding (ZZ) and His10 tags, both tags can be cleaved by rhinovirus 3C protease and His 10 tag is tested to show bands for Western Blot. The ZMPSTE24 gene is missing the codon for the normal C-terminal histidine. The yeast stains YO1361 and YO1362 were stored at -80°C in Prof. Trempe lab in Mclntyre Medical Sciences Building. The yeast stains were cultured in Prof. Berghuis lab in Francesco Bellini Life Sciences Building.

3.3.2 ZMPSTE24 expression

The human transmembrane protease, ZMPSTE24, was expressed in baker's yeast *S. cerevisiae*. First, pipette tips are used to pick a small amount of YO1362 strain from tubes. Then cells were added the yeast strain in the 100 ml of liquid yeast extract peptone dextrose (YPD) medium in a flask. The mini culture was incubated in an incubating shaker at 30°C while shaking at 230 rpm for 24 h.

After the mini culture, the cultured yeast strain and YPD media were added to 1 L selection medium, SD-Ura media, to culture in an incubating shaker at 30°C while shaking at 230 rpm until their OD_{600} reached 2.0. The cell cultures were centrifuged at 4000 × g for 10 min at 4°C.

The pellets from SD-Ura media were collected and did further culture in a BioFlo 3000 fermenter. The yeast strains were cultivated at 26°C, pH 5.0 with agitation at 400 rpm in fermenter. The expression of ZMPSTE24 was induced after carbon source depletion from YPD medium. Cells were harvested after 24 h incubation and 24 h protein expression, the concentration of yeast was tested until its OD_{600} reached 14. The pH of yeast culture was confirmed by pH sensor. After the expression of ZMPSTE24, cells were centrifuged at 5000 rpm for 20 min at 4°C and then the pellets were stored at -80°C.

3.3.3 Cell lysis

The cells were transferred from -80°C and induced cell recovery at 4°C. After thawing at 4°C, cells were resuspended in tubes with lysis buffer (cell wet weight: buffer = 1g: 1ml). I used Avestin C-5 homogenizer to lyse yeast pellets twice at around 10, 000 psi in Bellini Building. The buffer of resuspended pellets needs to be kept at 4°C to prevent rapid degradation and denaturation of proteins. After homogenizing step, the lysing solution was centrifuged at 4000 × g for 10 min at 4°C. The pellets were collected and resuspend in lysis buffer. The pellets were homogenized again through homogenizer at around 10, 000 psi twice again. The lysing solution was centrifuged at 4000 × g for 12 min at 4°C. Then pellets were resuspended in lysis buffer and were homogenized twice (under the same conditions as the previous passes), then centrifuged again at 4000 × g for 12 min at 4°C.

The pellets which contained membranes were isolated from the supernatant by ultracentrifuge at 120,000 × g for 1 h at 4°C. The pellets with crude membrane were resuspended in lysis buffer. The lysis buffer was added 20% (w/v) DDM detergent to a final detergent concentration of 1.5% (w/v) as solution buffer. The crude membrane was incubated with the solution buffer on a roller-mixer at room temperature for 90 min. Finally, the solution was centrifuged at 4000 × g for 20 min at 4°C, the insoluble protein and membrane was removed.

3.3.4 Protein purification

The protein purification steps were all performed at 4°C to prevent rapid degradation and denaturation of proteins. The C-terminal IgG-binding tag was used in the ZMPSTE24 purification steps. The IgG Sepharose 6 Fast Flow Affinity Resin was pre-equilibrated with water and IgG-binding buffer by centrifuging three times at 700 × g for 3 min at 4°C. The crude membranes solution was incubated with IgG Sepharose resin on a roller-mixer for 4 h. After the IgG incubation step, the IgG Sepharose resin was washed with 30 resin volumes wash buffer four times by centrifuging at 700 × g for 3 min at 4°C in 50 ml falcon tubes.

The protein ZMPSTE24 was removed from IgG resin on cleavage step by cleaving the tag using rhinovirus 3C protease. The IgG Sepharose resin was incubated with one volume wash buffer, and 1 mg rhinovirus 3C protease overnight at 4°C. The membrane ZMPSTE24 which contained C-terminal ZZ-tag was separated from this cleavage step. Then the rhinovirus 3C protease which contained C-terminal His-tag was separated by Immobilized Chelate Affinity Chromatography (ICMT) step.

The rhinovirus 3C protease was solubilized in solution and was removed by nickel affinity resin. The resin was pre-equilibrated with water and wash buffer by centrifuging three times at 700 × g for 3 min at 4°C. The tagged 3C protease was removed by incubation of the filter with 1 mL of nickel affinity resin for 2 h. The protein ZMPSTE24 was collected in the supernatant and then concentrated to 5 mL by 50 kDa centrifugal concentrator.

After the ICMT step, the protein was additionally purified by size elution chromatography to remove the aggregated protein and other proteins. The Superdex 200 16/600 column was pre-equilibrated with water and gel filtration buffer at a flow rate of 1 mL/min. The protein ZMPSTE24

was eluted with gel filtration buffer at a flow rate of 0.8 mL/min. Each fraction contained 2.5 mL liquids. I collected the protein fractions from the protein peak B were combined and concentrated with 30 kDa centrifugal concentrator. The protein was collected and divided in 10 aliquots. ZMPSTE24 should be analyzed in further experiments immediately or stored at -80°C.

3.3.5 MALDI analysis

After the size elution chromatography, the exist of ZMPSTE24 was confirmed by MALDI analysis. MALDI analysis is an ionization technique that uses a laser energy absorbing matrix to create ions from large molecules with minimal fragmentation.

First, the C18 desalting column was activated by 50% methanol (200 ul), then the column resin was equilibrated by 5% acetonitrile and 0.5% trifluoroacetic acid (TFA) solution. Two steps should spin at 1, 000 × g for 3 min. Then adding 100 uL aliquot solution on the column, the sample was centrifuged twice at 1, 000 × g for 4 min. After the binding step, the column was washed by 5% ACN (with 0.5% TFA). The column was centrifuged three times at 1, 000 × g for 5 min. Finally, the protein was eluted from the resin by using 70% ACN solution. The sample was centrifuged twice at 1, 000 × g for 3 min.

After the desalting preparation of protein ZMPSTE24, the solution for MALDI analysis should be prepared. In this experiment, the DHB matrix was used in the solution of MALDI analysis. DHB is insensitive to contaminations by salts and extra proteins. Spectra from single crystal preparations taken at threshold irradiance are free of matrix signals in the low mass range. The samples were spotted 1:1 with DHB matrix on a polished steel target and analyzed in linear-positive ionization mode (500 shots x 4 = 2,000 shots total per sample).

3.3.6 Mass spectrometry analysis

After the purification steps, the exist of protein ZMPSTE24 was analysed by native mass spectrometry (MS). The protein solution was transferred from -80°C and induced protein recovery at 4°C. The protein was exchanged from gel filtration buffer to mass spectrometry buffer by spin desalting column to do MS analysis.

The micro desalting column was centrifuged at 1, 000 × g for 2 min at 4°C to remove the previous buffer. The mass spectrometry buffer was added to the micro desalting column and centrifuged at 1, 000 × g for 1 min at 4°C four times to pre-equilibrate the column at first. The aliquot of sample was transferred from -80°C and added to the micro desalting column, and the column was centrifuged at 1, 500 × g for 5 min at 4°C. The concentration of ZMPSTE24 was re-confirmed by after the buffer exchange step by spectrometer.

The native MS experiment was done in Prof. Thibodeaux lab. The ZMPSTE24 MS solution was added into a modified quadrupole time-of-flight (QToF) mass spectrometer using gold-coated glass needles, and spectra were recorded under the following conditions: capillary, cone and collision cell voltages of 1.4 kV, 50 V and 150 V, respectively. The backing pressure was set to 0.5 mbar at first, and the pressure was added to 1.0 mbar.

Reference

1. Hampton, S. E.; Dore, T. M.; Schmidt, W. K., Rce1: mechanism and inhibition. *Crit Rev Biochem Mol Biol* **2018,** *53* (2), 157-174.

2. Gao, J.; Liao, J.; Yang, G. Y., CAAX-box protein, prenylation process and carcinogenesis. *Am J Transl Res* **2009,** *1* (3), 312-325.

3. Appels, N. M.; Beijnen, J. H.; Schellens, J. H., Development of farnesyl transferase inhibitors: a review. *Oncologist* **2005,** *10* (8), 565-578.

4. Spear, E. D.; Hsu, E. T.; Nie, L.; Carpenter, E. P.; Hrycyna, C. A.; Michaelis, S., ZMPSTE24 missense mutations that cause progeroid diseases decrease prelamin A cleavage activity and/or protein stability. *Dis Model Mech* **2018,** *11* (7).

5. Young, S. G.; Meta, M.; Yang, S. H.; Fong, L. G., Prelamin A farnesylation and progeroid syndromes. *J Biol Chem* **2006,** *281* (52), 39741-39745.

6. Zhu, D.; Wu, Q.; Hua, L., 3.01 - Industrial Enzymes. In *Comprehensive Biotechnology (Third Edition)*, Moo-Young, M., Ed. Pergamon: Oxford, 2019; pp 1-13.

7. Auld, D. S., Metalloproteases. In *Encyclopedia of Biological Chemistry (Second Edition)*, Lennarz, W. J.; Lane, M. D., Eds. Academic Press: Waltham, 2013; pp 86-89.

8. Jongeneel, C. V.; Bouvier, J.; Bairoch, A., A unique signature identifies a family of zinc-dependent metallopeptidases. *FEBS Lett* **1989,** *242* (2), 211-214.

9. Adekoya, O. A.; Sylte, I., The Thermolysin Family (M4) of Enzymes: Therapeutic and Biotechnological Potential. *Chem Biol Drug Des* **2009,** *73* (1), 7-16.

10. Pryor, E. E., Jr.; Horanyi, P. S.; Clark, K. M.; Fedoriw, N.; Connelly, S. M.; Koszelak-Rosenblum, M.; Zhu, G.; Malkowski, M. G.; Wiener, M. C.; Dumont, M. E., Structure of the integral membrane protein CAAX protease Ste24p. *Science* **2013,** *339* (6127), 1600-1604.

11. Matthews, B. W., Structural basis of the action of thermolysin and related zinc peptidases. *Accounts Chem Res* **1988,** *21* (9), 333-340.

12. Feder, J.; Schuck, J. M., Studies on the Bacillus subtilis neutral-protease- and Bacillus thermoproteolyticus thermolysin-catalyzed hydrolysis of dipeptide substrates. *Biochemistry* **1970,** *9* (14), 2784-2791.

13. Colman, P. M.; Jansonius, J. N.; Matthews, B. W., The structure of thermolysin: An electron density map at 2.3 Å resolution. *J Mol Biol* **1972,** *70* (3), 701-724.

14. Weaver, L. H.; Kester, W. R.; Matthews, B. W., A crystallographic study of the complex of phosphoramidon with thermolysin. A model for the presumed catalytic transition state and for the binding of extended substances. *J Mol Biol* **1977,** *114* (1), 119-132.

15. Hausrath, A. C.; Matthews, B. W., Thermolysin in the absence of substrate has an open conformation. *Acta Crystallogr D Biol Crystallogr* **2002,** *58* (6-2), 1002-1007.

16. van den Burg, B.; Eijsink, V., Chapter 111 - Thermolysin and Related Bacillus Metallopeptidases. In *Handbook of Proteolytic Enzymes (Third Edition)*, Rawlings, N. D.; Salvesen, G., Eds. Academic Press: 2013; pp 540-553.

17. Pozsgay, M.; Michaud, C.; Liebman, M.; Orlowski, M., Substrate and inhibitor studies of thermolysin-like neutral metalloendopeptidase from kidney membrane fractions. Comparison with bacterial thermolysin. *Biochemistry* **1986,** *25* (6), 1292-1299.

18. Heinrikson, R. L., Applications of thermolysin in protein structural analysis. *Methods Enzymol* **1977,** *47*, 175-189.

19. Holmquist, B.; Vallee, B. L., Metal substitutions and inhibition of thermolysin: spectra of the cobalt enzyme. *J Biol Chem* **1974,** *249* (14), 4601-4607.

20. Holland, D. R.; Hausrath, A. C.; Juers, D.; Matthews, B. W., Structural analysis of zinc substitutions in the active site of thermolysin. *Protein Sci* **1995,** *4* (10), 1955-1965.

21. Fontana, A., Structure and stability of thermophilic enzymes. Studies on thermolysin. *Biophys Chem* **1988,** *29* (1-2), 181-193.

22. Roche, R. S.; Voordouw, G., The structural and functional roles of metal ions in thermolysin. *CRC Crit Rev Biochem* **1978,** *5* (1), 1-23.

23. Matthews, B. W.; Weaver, L. H., Binding of lanthanide ions to thermolysin. *Biochemistry* **1974,** *13* (8), 1719-1725.

24. Yang, H.; Yang, M.; Ding, Y.; Liu, Y.; Lou, Z.; Zhou, Z.; Sun, L.; Mo, L.; Ye, S.; Pang, H.; Gao, G. F.; Anand, K.; Bartlam, M.; Hilgenfeld, R.; Rao, Z., The crystal structures of severe acute respiratory syndrome virus main protease and its complex with an inhibitor. *Proc Natl Acad Sci U S A* **2003,** *100* (23), 13190-13195.

25. Zhang, L.; Lin, D.; Sun, X.; Curth, U.; Drosten, C.; Sauerhering, L.; Becker, S.; Rox, K.; Hilgenfeld, R., Crystal structure of SARS-CoV-2 main protease provides a basis for design of improved α-ketoamide inhibitors. *Science* **2020,** *368* (6489), 409-412.

26. Goblirsch, B. R.; Arachea, B. T.; Councell, D. J.; Wiener, M. C., Phosphoramidon inhibits the integral membrane protein zinc metalloprotease ZMPSTE24. *Acta Crystallogr D Struct Biol* **2018,** *74* (8), 739-747.

27. Hangauer, D. G.; Monzingo, A. F.; Matthews, B. W., An interactive computer graphics study of thermolysin-catalyzed peptide cleavage and inhibition by N-carboxymethyl dipeptides. *Biochemistry* **1984,** *23* (24), 5730-5741.

28. Beaumont, A.; O'Donohue, M. J.; Paredes, N.; Rousselet, N.; Assicot, M.; Bohuon, C.; Fournié-Zaluski, M.-C.; Roques, B. P., The Role of Histidine 231 in Thermolysin-like Enzymes.: A SITE-DIRECTED MUTAGENESIS STUDY. *J Biol Chem* **1995,** *270* (28), 16803-16808.

29. Kubo, M.; Mitsuda, Y.; Takagi, M.; Imanaka, T., Alteration of specific activity and stability of thermostable neutral protease by site-directed mutagenesis. *Appl Environ Microb* **1992,** *58* (11), 3779-3783.

30. Toma, S.; Campagnoli, S.; De Gregoriis, E.; Gianna, R.; Margarit, I.; Zamai, M.; Grandi, G., Effect of Glu-143 and His-231 substitutions on the catalytic activity and secretion of Bacillus subtilis neutral protease. *Protein Eng* **1989,** *2* (5), 359-364.

31. Roques, B. P.; Noble, F.; Daugé, V.; Fournié-Zaluski, M. C.; Beaumont, A., Neutral endopeptidase 24.11: structure, inhibition, and experimental and clinical pharmacology. *Pharmacol Rev* **1993,** *45* (1), 87-146.

32. Vriend, G.; Eijsink, V., Prediction and analysis of structure, stability and unfolding of thermolysin-like proteases. *J Comput Aided Mol Des* **1993,** *7* (4), 367-396.

33. Tam, A.; Nouvet, F. J.; Fujimura-Kamada, K.; Slunt, H.; Sisodia, S. S.; Michaelis, S., Dual roles for Ste24p in yeast a-factor maturation: NH2-terminal proteolysis and COOH-terminal CAAX processing. *J Cell Biol* **1998,** *142* (3), 635-649.

34. Hildebrandt, E. R.; Arachea, B. T.; Wiener, M. C.; Schmidt, W. K., Ste24p Mediates Proteolysis of Both Isoprenylated and Non-prenylated Oligopeptides. *J Biol Chem* **2016,** *291* (27), 14185-14198.

35. Corrigan, D. P.; Kuszczak, D.; Rusinol, A. E.; Thewke, D. P.; Hrycyna, C. A.; Michaelis, S.; Sinensky, M. S., Prelamin A endoproteolytic processing in vitro by recombinant Zmpste24. *Biochem J* **2005,** *387* (1), 129-138.

36. Young, S. G.; Fong, L. G.; Michaelis, S., Prelamin A, Zmpste24, misshapen cell nuclei, and progeria--new evidence suggesting that protein farnesylation could be important for disease pathogenesis. *J Lipid Res* **2005,** *46* (12), 2531-2558.

37. Hsu, E. T.; Vervacke, J. S.; Distefano, M. D.; Hrycyna, C. A., A Quantitative FRET Assay for the Upstream Cleavage Activity of the Integral Membrane Proteases Human ZMPSTE24 and Yeast Ste24. *Methods Mol Biol* **2019,** *2009*, 279-293.

38. Mehmood, S.; Marcoux, J.; Gault, J.; Quigley, A.; Michaelis, S.; Young, S. G.; Carpenter, E. P.; Robinson, C. V., Mass spectrometry captures off-target drug binding and provides mechanistic insights into the human metalloprotease ZMPSTE24. *Nat Chem* **2016,** *8* (12), 1152-1158.

39. Manolaridis, I.; Kulkarni, K.; Dodd, R. B.; Ogasawara, S.; Zhang, Z.; Bineva, G.; Reilly, N. O.; Hanrahan, S. J.; Thompson, A. J.; Cronin, N.; Iwata, S.; Barford, D., Mechanism of farnesylated CAAX protein processing by the intramembrane protease Rce1. *Nature* **2013,** *504* (7479), 301-305.

40. Clark, K. M.; Jenkins, J. L.; Fedoriw, N.; Dumont, M. E., Human CaaX protease ZMPSTE24 expressed in yeast: Structure and inhibition by HIV protease inhibitors. *Protein Sci* **2017,** *26* (2), 242-257.

41. de la Rosa, J.; Freije, J. M.; Cabanillas, R.; Osorio, F. G.; Fraga, M. F.; Fernandez-Garcia, M. S.; Rad, R.; Fanjul, V.; Ugalde, A. P.; Liang, Q.; Prosser, H. M.; Bradley, A.; Cadinanos, J.; Lopez-Otin, C., Prelamin A causes progeria through cell-extrinsic mechanisms and prevents cancer invasion. *Nat Commun* **2013,** *4*, 2268.

42. Liu, B.; Wang, J.; Chan, K. M.; Tjia, W. M.; Deng, W.; Guan, X.; Huang, J. D.; Li, K. M.; Chau, P. Y.; Chen, D. J.; Pei, D.; Pendas, A. M.; Cadiñanos, J.; López-Otín, C.; Tse, H. F.; Hutchison, C.; Chen, J.; Cao, Y.; Cheah, K. S.; Tryggvason, K.; Zhou, Z., Genomic instability in laminopathy-based premature aging. *Nat Med* **2005,** *11* (7), 780-785.

43. Fu, B.; Wang, L.; Li, S.; Dorf, M. E., ZMPSTE24 defends against influenza and other pathogenic viruses. *J Exp Med* **2017,** *214* (4), 919-929.

44. Mehmood, S.; Marcoux, J.; Gault, J.; Quigley, A.; Michaelis, S.; Young, S. G.; Carpenter, E. P.; Robinson, C. V., Mass spectrometry captures off-target drug binding and provides mechanistic insights into the human metalloprotease ZMPSTE24. *Nat Chem* **2016,** *8* (12), 1152-1158.

45. Quigley, A.; Dong, Y. Y.; Pike, A. C.; Dong, L.; Shrestha, L.; Berridge, G.; Stansfeld, P. J.; Sansom, M. S.; Edwards, A. M.; Bountra, C.; von Delft, F.; Bullock, A. N.; Burgess-Brown, N. A.; Carpenter, E. P., The structural basis of ZMPSTE24-dependent laminopathies. *Science* **2013,** *339* (6127), 1604-1607.

46. Tonoyama, Y.; Shinya, M.; Toyoda, A.; Kitano, T.; Oga, A.; Nishimaki, T.; Katsumura, T.; Oota, H.; Wan, M. T.; Yip, B. W. P.; Helen, M. O. L.; Chisada, S.; Deguchi, T.; Au, D. W. T.; Naruse, K.; Kamei, Y.; Taniguchi, Y., Abnormal nuclear morphology is independent of longevity in a zmpste24-deficient fish model of Hutchinson-Gilford progeria syndrome (HGPS). *Comp Biochem Physiol C Toxicol Pharmacol* **2018,** *209*, 54-62.

47. Varela, I.; Cadinanos, J.; Pendas, A. M.; Gutierrez-Fernandez, A.; Folgueras, A. R.; Sanchez, L. M.; Zhou, Z.; Rodriguez, F. J.; Stewart, C. L.; Vega, J. A.; Tryggvason, K.; Freije, J. M.; Lopez-Otin, C., Accelerated ageing in mice deficient in Zmpste24 protease is linked to p53 signalling activation. *Nature* **2005,** *437* (7058), 564-568.

48. Bergo, M. O.; Gavino, B.; Ross, J.; Schmidt, W. K.; Hong, C.; Kendall, L. V.; Mohr, A.; Meta, M.; Genant, H.; Jiang, Y.; Wisner, E. R.; Van Bruggen, N.; Carano, R. A.; Michaelis, S.; Griffey, S. M.; Young, S. G., Zmpste24 deficiency in mice causes spontaneous bone fractures, muscle weakness, and a prelamin A processing defect. *Proc Natl Acad Sci U S A* **2002,** *99* (20), 13049-13054.

49. Eriksson, M.; Brown, W. T.; Gordon, L. B.; Glynn, M. W.; Singer, J.; Scott, L.; Erdos, M. R.; Robbins, C. M.; Moses, T. Y.; Berglund, P.; Dutra, A.; Pak, E.; Durkin, S.; Csoka, A. B.; Boehnke, M.; Glover, T. W.; Collins, F. S., Recurrent de novo point mutations in lamin A cause Hutchinson-Gilford progeria syndrome. *Nature* **2003,** *423* (6937), 293-298.

50. Bonne, G.; Di Barletta, M. R.; Varnous, S.; Becane, H. M.; Hammouda, E. H.; Merlini, L.; Muntoni, F.; Greenberg, C. R.; Gary, F.; Urtizberea, J. A.; Duboc, D.; Fardeau, M.; Toniolo, D.; Schwartz, K., Mutations in the gene encoding lamin A/C cause autosomal dominant Emery-Dreifuss muscular dystrophy. *Nat Genet* **1999,** *21* (3), 285-288.

51. Dalton, M.; Sinensky, M., Expression systems for nuclear lamin proteins: farnesylation in assembly of nuclear lamina. *Methods Enzymol* **1995,** *250*, 134-148.

52. Diociaiuti, A.; D'Amico, P.; Pisaneschi, E.; Giancristoforo, S.; Pappalardo, M. G.; Di Guardo, V.; Zambruno, G.; El Hachem, M., Teledermatology diagnosis of the first Italian patient affected with restrictive dermopathy due to ZMPSTE24 homozygous mutation. *J Eur Acad Dermatol Venereol* **2019,** *33* (3), e139-e140.

53. Novelli, G.; Muchir, A.; Sangiuolo, F.; Helbling-Leclerc, A.; D'Apice, M. R.; Massart, C.; Capon, F.; Sbraccia, P.; Federici, M.; Lauro, R.; Tudisco, C.; Pallotta, R.; Scarano, G.; Dallapiccola, B.; Merlini, L.; Bonne, G., Mandibuloacral dysplasia is caused by a mutation in LMNA-encoding lamin A/C. *Am J Hum Genet* **2002,** *71* (2), 426-431.

54. Ullrich, N. J.; Gordon, L. B., Hutchinson-Gilford progeria syndrome. *Handb Clin Neurol* **2015,** *132*, 249-264.

55. Prakash, A.; Gordon, L. B.; Kleinman, M. E.; Gurary, E. B.; Massaro, J.; D'Agostino, R., Sr.; Kieran, M. W.; Gerhard-Herman, M.; Smoot, L., Cardiac Abnormalities in Patients With Hutchinson-Gilford Progeria Syndrome. *JAMA Cardiol* **2018,** *3* (4), 326-334.

56. Moiseeva, O.; Lessard, F.; Acevedo-Aquino, M.; Vernier, M.; Tsantrizos, Y. S.; Ferbeyre, G., Mutant lamin A links prophase to a p53 independent senescence program. *Cell Cycle* **2015,** *14* (15), 2408-2421.

57. Joerger, A. C.; Fersht, A. R., The p53 Pathway: Origins, Inactivation in Cancer, and Emerging Therapeutic Approaches. *Annu Rev Biochem* **2016,** *85*, 375-404.

58. Coffinier, C.; Hudon, S. E.; Farber, E. A.; Chang, S. Y.; Hrycyna, C. A.; Young, S. G.; Fong, L. G., HIV protease inhibitors block the zinc metalloproteinase ZMPSTE24 and lead to an accumulation of prelamin A in cells. *Proc Natl Acad Sci U S A* **2007,** *104* (33), 13432-13437.

59. Toth, J. I.; Yang, S. H.; Qiao, X.; Beigneux, A. P.; Gelb, M. H.; Moulson, C. L.; Miner, J. H.; Young, S. G.; Fong, L. G., Blocking protein farnesyltransferase improves nuclear shape in fibroblasts from humans with progeroid syndromes. *Proc Natl Acad Sci U S A* **2005,** *102* (36), 12873-12878.

60. López-Otín, C.; Hunter, T., The regulatory crosstalk between kinases and proteases in cancer. *Nat Rev Cancer* **2010,** *10* (4), 278-292.

61. Flexner, C., HIV-protease inhibitors. *N Engl J Med* **1998,** *338* (18), 1281-1292.

62. Matralis, A. N.; Xanthopoulos, D.; Huot, G.; Lopes-Paciencia, S.; Cole, C.; de Vries, H.; Ferbeyre, G.; Tsantrizos, Y. S., Molecular tools that block maturation of the nuclear lamin A and decelerate cancer cell migration. *Bioorg Med Chem* **2018,** *26* (20), 5547-5554.

63. Coffinier, C.; Hudon, S. E.; Lee, R.; Farber, E. A.; Nobumori, C.; Miner, J. H.; Andres, D. A.; Spielmann, H. P.; Hrycyna, C. A.; Fong, L. G.; Young, S. G., A potent HIV protease inhibitor, darunavir, does not inhibit ZMPSTE24 or lead to an accumulation of farnesyl-prelamin A in cells. *J Biol Chem* **2008,** *283* (15), 9797-9804.

64. Goulbourne, C. N.; Vaux, D. J., HIV protease inhibitors inhibit FACE1/ZMPSTE24: a mechanism for acquired lipodystrophy in patients on highly active antiretroviral therapy. *Biochem Soc Trans* **2010,** *38* (1), 292-296.

65. Yang, S. H.; Chang, S. Y.; Ren, S.; Wang, Y.; Andres, D. A.; Spielmann, H. P.; Fong, L. G.; Young, S. G., Absence of progeria-like disease phenotypes in knock-in mice expressing a non-farnesylated version of progerin. *Hum Mol Genet* **2011,** *20* (3), 436-444.

66. Waller, D. D.; Park, J.; Tsantrizos, Y. S., Inhibition of farnesyl pyrophosphate (FPP) and/or geranylgeranyl pyrophosphate (GGPP) biosynthesis and its implication in the treatment of cancers. *Crit Rev Biochem Mol Biol* **2019,** *54* (1), 41-60.

67. Chang, S. Y.; Hudon-Miller, S. E.; Yang, S. H.; Jung, H. J.; Lee, J. M.; Farber, E.; Subramanian, T.; Andres, D. A.; Spielmann, H. P.; Hrycyna, C. A.; Young, S. G.; Fong, L. G., Inhibitors of protein geranylgeranyltransferase-I lead to prelamin A accumulation in cells by inhibiting ZMPSTE24. *J Lipid Res* **2012,** *53* (6), 1176-1182.

68. Bikkul, M. U.; Clements, C. S.; Godwin, L. S.; Goldberg, M. W.; Kill, I. R.; Bridger, J. M., Farnesyltransferase inhibitor and rapamycin correct aberrant genome organisation and

decrease DNA damage respectively, in Hutchinson-Gilford progeria syndrome fibroblasts. *Biogerontology* **2018,** *19* (6), 579-602.

69. Lee, K. M.; DaSilva, N. A., Evaluation of the Saccharomyces cerevisiae ADH2 promoter for protein synthesis. *Yeast* **2005,** *22* (6), 431-440.

70. Chen, C.; Huang, Q. L.; Jiang, S. H.; Pan, X.; Hua, Z. C., Immobilized protein ZZ, an affinity tool for immunoglobulin isolation and immunological experimentation. *Biotechnol Appl Biochem* **2006,** *45* (2), 87-92.